Chemical Science

ROYAL SOCIETY OF CHEMISTRY

PERSPECTIVE

View Article Online
View Journal | View Issue

Cite this: *Chem. Sci.*, 2025, **16**, 17034

All publication charges for this article have been paid for by the Royal Society of Chemistry

Received 19th July 2025
Accepted 2nd September 2025

DOI: 10.1039/d5sc05394c

rsc.li/chemical-science

Multicomponent covalent organic frameworks: design strategies and synergistic functions

Xiaoyi Xu and Ning Huang *

Covalent organic frameworks (COFs) are crystalline porous polymers with modular architectures and long-range order, offering exceptional tunability in pore structure and functionality. While conventional COFs are typically constructed from one or two types of monomers, recent advances have led to the emergence of multicomponent COFs (MC-COFs), which integrate three or more distinct building blocks within a single lattice. This strategy enables the precise spatial arrangement of diverse geometries, connectivity, and functionalities, imparting synergistic complexity beyond the reach of single- or binary-component systems. In this perspective, we present a comprehensive overview of MC-COF chemistry, organised around five representative construction strategies: isostructural and heterostructural copolymerization, multicomponent topological design, multicomponent reactions, and pore partitioning strategies. We further highlight how these frameworks enable emergent functions in catalysis, alkane isomer separation, chemical sensing, and radiotherapy through rational control of both periodic backbone structure and local chemical environments. Despite these advances, challenges persist in structural characterization, expanding the scope of dynamic linkages, and achieving predictive design of emergent properties. Looking forward, the integration of dynamic covalent chemistry, topological programming, and machine learning-driven design is expected to unlock the full potential of MC-COFs as next-generation multifunctional materials.

1 Introduction

Covalent Organic Frameworks (COFs) have emerged as a family of crystalline porous polymers constructed through covalent linkages between precisely designed organic building blocks.[1–3] Since their inaugural synthesis in 2005,[4] COFs have garnered

State Key Laboratory of Silicon and Advanced Semiconductor Materials, Department of Polymer Science and Engineering, Zhejiang University, Hangzhou 310058, China. E-mail: nhuang@zju.edu.cn

Xiaoyi Xu

Xiaoyi Xu received his Bachelor's degree from Soochow University in 2018, his Master's degree from National University of Singapore in 2019, and his PhD degree from Zhejiang University in 2025. After that, he started his postdoctoral research at Zhejiang University. His current scientific interests are focused on the design and synthesis of semiconducting COFs.

Ning Huang

Ning Huang is a professor in Department of Polymer Science and Engineering, Zhejiang University. He received his BS degree from Shandong University in 2009 and PhD degree from Institute of Molecular Sciences (Japan) in 2015. From 2016 to 2019, he worked as a postdoctoral researcher in Japan Advanced Institute of Science and Technology, Texas A&M University, and National University of Singapore. In 2019, he started a faculty position in Zhejiang University. His research interests include the design, synthesis, and function exploration of crystalline two-dimensional polymers, including covalent organic frameworks and metal–organic frameworks.

significant interest within the porous materials community due to their exceptional structural tunability, programmable topologies, high surface areas, and remarkable chemical stability.[5–7] The precise incorporation of functional moieties within their periodic architectures has enabled COFs to demonstrate exceptional potential across diverse frontier domains, including heterogeneous catalysis,[8–10] gas separation,[11–13] energy storage systems,[14–16] optoelectronic devices,[17,18] and chemical sensing platforms.[19,20]

Despite remarkable advances in COF chemistry, the structural complexity of most reported systems remains constrained by synthetic paradigms relying on single-monomer self-polymerization or binary condensation of two complementary units. These conventional approaches fall short in achieving precise pore environment customization and framework structural diversity, thereby hindering their capacity to address the growing requirements of sophisticated multifunctional applications. In stark contrast, nature's macromolecular masterpieces—DNA helices, protein quaternary assemblies and beyond—attain unprecedented functional sophistication through the orchestrated interplay of multiple, distinct components. COFs, with their inherent capacity for spatial precision in framework engineering, establish an ideal platform for constructing structurally sophisticated multicomponent architectures through programmable covalent connectivity. Their crystalline lattices enable deterministic positioning of functional building blocks, enabling the creation of hierarchically ordered systems where molecular-scale design principles synergize with diverse mesoscale functionalities. This unique capability positions COFs at the forefront of addressing the fundamental challenge in materials science: reconciling long-range structural order with multifunctional complexity.

Driven by this innovative paradigm, this field has embarked on pioneering the development of multicomponent covalent organic frameworks (MC-COFs), which are defined as highly ordered crystalline networks intricately woven from three or more precisely stoichiometrically prescribed monomers. Harnessing the inherent reversibility and error-correction of dynamic covalent chemistry, MC-COFs achieve precise control over monomer ratios and their spatial arrangement within the lattice. Unlike mere doped composites or physical blends, these MC-COFs structurally integrate complementary functional elements into an ordered framework, thereby giving rise to emergent properties that surpass the simple summation of their individual components. Embracing this vision, the deliberate incorporation of additional monomers in MC-COFs serves a dual purpose: topologically, these components sculpt pore architectures, fine-tuning dimensions, shapes, and connectivity, and even engendering novel COFs topologies with distinct porosity profiles; functionally, they introduce bespoke active sites and microenvironmental niches tailored to specific chemical tasks.

Current research is centered on elucidating the mechanisms of dynamic covalent co-condensation to enable precise multicomponent integration and multiscale structural validation. Meanwhile, it systematically explores the structure–property relationship underlying the emergent porosity and framework functionalities of MC-COFs, which are intrinsic to their hierarchical architectures. By carefully selecting monomers and optimizing synthesis conditions, researchers can achieve atom-precise control over monomer ratios and spatial arrangement, thus unlocking a harmonious interplay between structural order and compositional diversity. This methodology not only expands the spectrum of accessible porous structures but also endows the framework with emergent host–guest interactions, catalytic performance, and selective binding affinities, capabilities that are unparalleled by any single- or dual-component COFs.

This perspective provides a comprehensive overview of MC-COFs, encompassing their structural characteristics, synthetic methodologies, and emerging applications. We first introduce the fundamental concepts of MC-COFs, including their building blocks and topological design principles. Next, we systematically elaborate on five key design strategies governing their construction, these developments have collectively delivered several conceptual and functional milestones (Fig. 1). Building upon this foundation, we elucidate how precisely engineered covalent connectivity and tailored pore

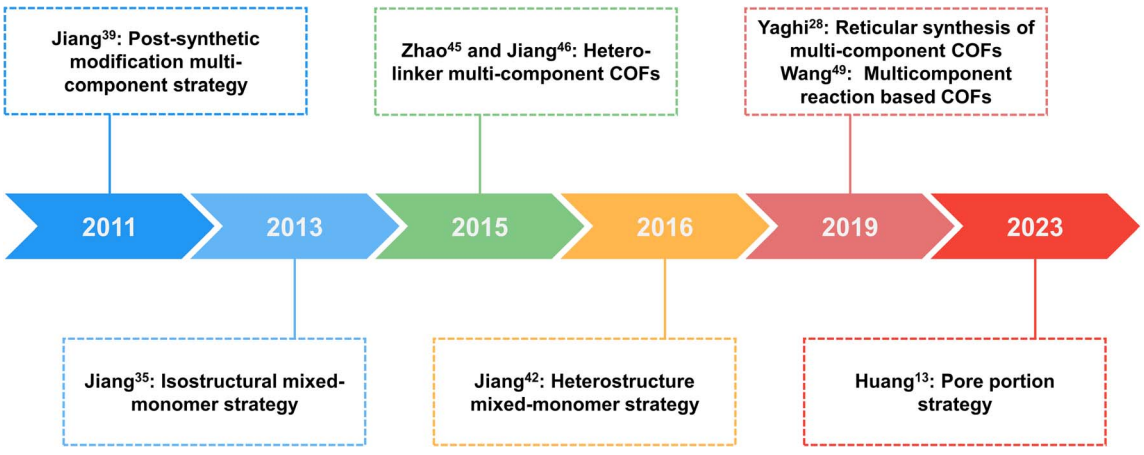

Fig. 1 Selected research milestones of MC-COFs.

microenvironments synergistically dictate functional performance across diverse domains, including heterogeneous catalysis,[21–23] alkane isomer separation,[13] light emission,[24] and chemical sensing.[25,26] Finally, we discuss future research directions and technical challenges in this field, with particular emphasis on MC-COFs' transformative potential in advancing next-generation multifunctional porous materials.

2 Structural cornerstones of MC-COFs

The construction of COFs is fundamentally grounded in three interconnected elements: topological design, building blocks, and linkages.[5] These elements operate in concert to dictate the architecture, porosity, crystallinity, stability and functional expression of the framework. In MC-COFs, the structural complexity and functional tunability are significantly enhanced by the modular integration of diverse components at each level.

Firstly, topological design serves as the blueprint of network growth, offering a conceptual map that governs how building units assemble into extended periodic structures. Topological diagrams define how covalent bonds should form in space, directing the orientation of each monomeric unit. By repeating a pre-defined geometric rule, the polymer chains propagate along specific crystallographic directions. The matching between the topological diagram and the symmetry of building blocks underpins the structural regularity and diversity of COFs. To date, the dual-component 2D COFs reported in the literature primarily comprise trigonal, tetragonal, pentagonal, or hexagonal pores with **hcb**, **sql**, **bex**, **kgm**, **hxl**, **kgd**, **mcm** topologies (Fig. 2a).[27] In MC-COFs, heterogeneity in node geometry, linker length, or symmetry enables the generation of complex and unconventional topologies, such as **tth**[28] and **mta**[13] nets (Fig. 2b). This multicomponent design paradigm enables the creation of frameworks with intricately tailored pore architectures and variable connectivity patterns that extend well beyond the reach of traditional binary systems.

Secondly, building blocks in COFs are generally planar, rigid, and π-conjugated, with well-defined symmetry. Hundreds of monomers have been developed to date, encompassing

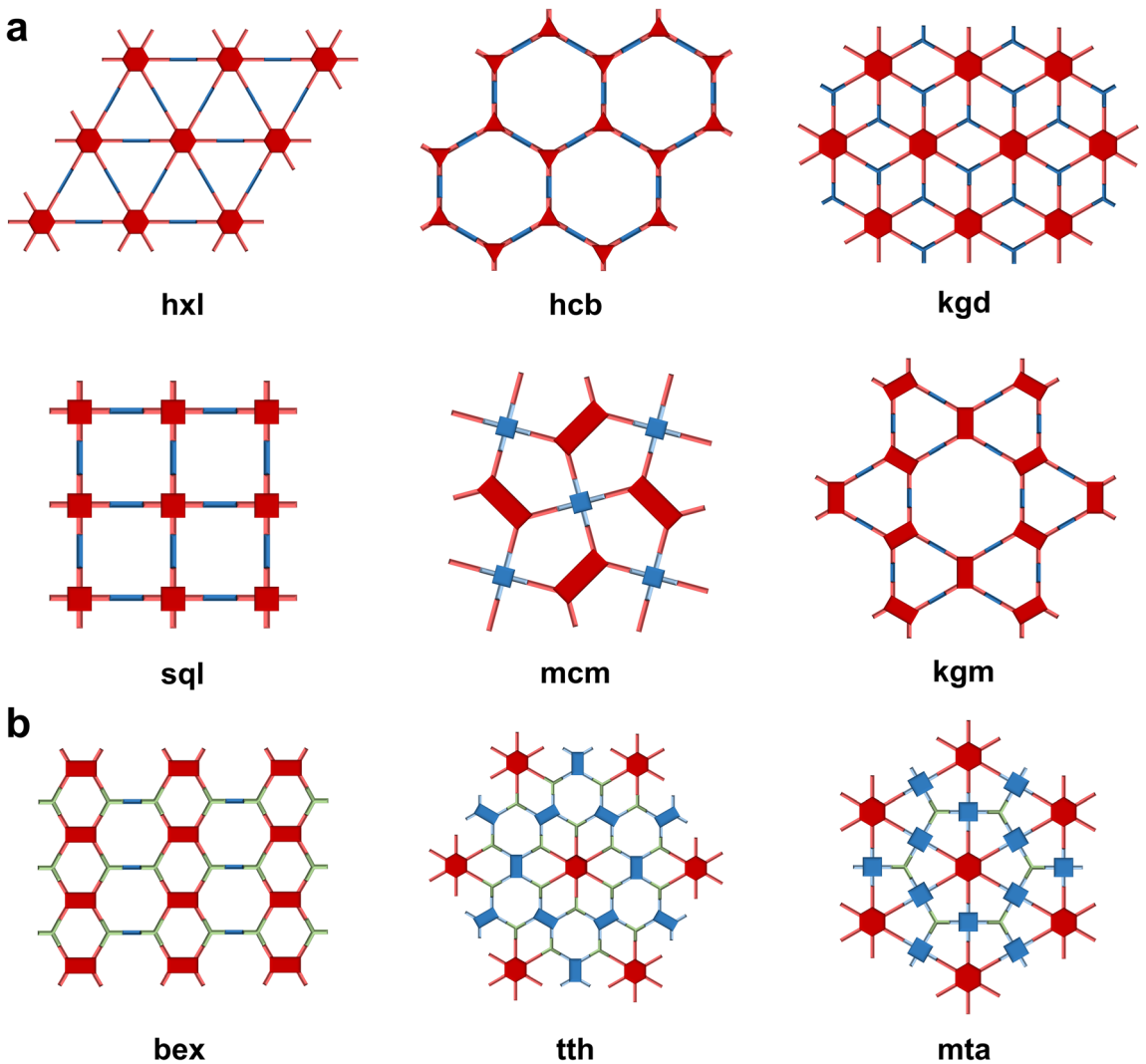

Fig. 2 Representative topologies for (a) 2D dual-component COFs and (b) MC-COFs.

benzene derivatives, heterocycles, macrocycles, and polycyclic aromatics.[29] In MC-COFs, the rational selection and combination of donor–acceptor (D–A) monomers introduces electronic complexity and functional synergy. Electron-rich donors, such as triphenylamine,[30–32] thiophene,[33–35] or carbazole,[36,37] promote charge mobility and photo-responsiveness. Acceptors like benzothiadiazole,[38–40] perylene diimide,[41–43] or triazine[31,44] enable energy-level tuning and charge delocalization. When integrated within a single framework, their spatial and electronic complementarity promotes intra-frame charge transfer and cooperative behaviours, which is a common method for two-component COFs, however this regulation is coarse. Notably, MC-COF provides a unique platform to enable fine tuning of electronic structures by introducing more component donors and acceptors, fabrication and synthesis of complex D–A architectures with tailored redox properties and enhanced optoelectronic response.

Lastly, linkage chemistry governs both the stability and the functional of COFs. Traditional dynamic linkages, such as boron[4] and imine,[45] are favoured for their reversible nature, promoting error correction and framework crystallinity. In contrast, emerging irreversible linkages like olefin,[46–48] phenazine[10,49] offer superior robustness and electronic conjugation, which are crucial for energy-related applications. The multicomponent design strategy further expands this domain: the coexistence or sequence control of different linkages in a single framework enables localised functionality and spatially resolved electronic features, enriching both structure and function.

In summary, topological design, building blocks, and linkage chemistry act synergistically to shape the architecture and properties of MC-COFs. Their interplay determines key attributes such as porosity, crystallinity, stability, and functionality.

3 Design strategies for MC-COFs

MC-COFs have been developed for over a decade. Based on the structural design of monomers and the development of COFs structures, many representative works have been proposed. In this perspective, according to the design concepts and objectives of multicomponent COFs, the methodology of multicomponent COFs is divided into the following five categories: isostructural mixed-monomer strategy, heterostructure mixed-monomer strategy, multicomponent topological design, multicomponent reactions, and pore portion strategy.

3.1 Isostructural mixed-monomer strategy

In the early development of COFs, although certain studies had successfully synthesized multicomponent systems, these materials were not yet formally recognized as a distinct subclass. Most early efforts focused on modulating the chemical environment within a fixed framework topology by incorporating functionally varied building blocks without altering the underlying lattice structure. One notable strategy, pioneered by the Jiang group, involved the co-assembly of linkers with identical length, size, and core architecture but bearing different peripheral substituents, yielding isostructural MC-COFs with tunable crystallinity and porosity.[50,51]

Specifically, they introduced fluoro-substituted and unsubstituted aromatic units into the edge positions of imine-linked porphyrin COFs in controlled molar ratios. This strategy not only enables the fine-tuning of self-complementary π–π interactions between electron-donating and electron-accepting linkers but also leads to the formation of anisotropic skeletons with optimized stacking geometry. Such structural anisotropy enhances framework-wide π-electron delocalization and facilitates directional charge transport along the stacked columns. As a result, these COFs exhibit narrowed HOMO–LUMO gaps and significantly improved light-harvesting performance (Fig. 3a).[50] The deliberate introduction of chemical heterogeneity thus directly contributes to enhanced electronic transmission and photophysical properties.

Building on this strategy, Jiang *et al.* further demonstrated that the intra-framework hydrogen-bonding landscape within 2D COFs could be precisely engineered through multicomponent condensation. Specifically, hydrogen-bonding motifs were introduced at the edge of imine-linked tetragonal porphyrin COFs and their content finely tuned *via* a three-component strategy (Fig. 3b).[51] This manipulation induced sheet planarization, strengthened interlayer interactions, and promoted extended π-conjugation, thereby improving crystallinity, porosity, and photo response. Importantly, the resulting frameworks exhibited reduced band gaps and markedly enhanced photocatalytic activity, especially in singlet oxygen generation. These effects were consistent across both free-base and metalloporphyrin analogues, underscoring the versatility and generality of hydrogen-bonding control in MC-COFs.

Collectively, these studies underscore how subtle intercomponent interactions, such as electronic modulation and hydrogen bonding, can be harnessed within isostructural MC-COFs to finely tailor energy band structures and photophysical properties, offering early but powerful insights into the functional scope of multicomponent design strategies in COF chemistry.

Building upon this isostructural mixed-monomer strategy, other studies have extended gradient modulation to post-synthetic modification (PSM).[52] Through click chemistry, third-component monomers, such as alkyl, ester, hydroxyl, carboxyl or amino functionalities, can be grafted onto pore surfaces in varying proportions, enabling continuous tuning of channel polarity, hydrophilicity and guest-binding affinity.[53–55] This versatile compositional control has proven invaluable for optimizing COF architectures as selective CO_2 adsorbents, the tailored surface chemistries of which enhance CO_2–framework interactions, driving high-performance capture and separation (Fig. 4).[53,56]

Even more elaborately, the incorporation of fullerene derivatives *via* covalent anchoring within the pore walls yields three-component donor–acceptor COFs that spatially segregate electron-rich and electron-deficient domains (Fig. 5a–c).[55] This architectural design creates irregular yet highly functional pore geometries, which not only provide confined environments for

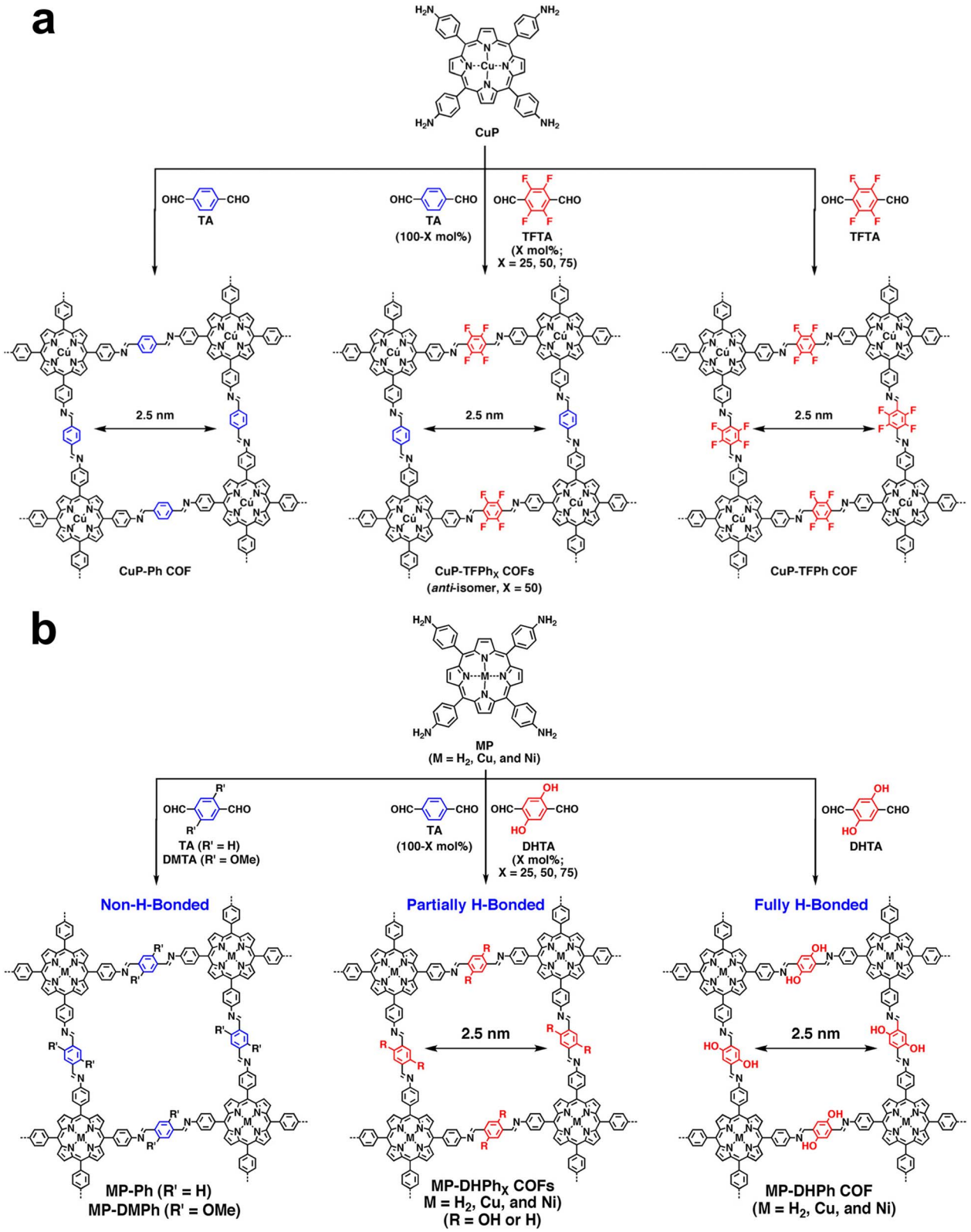

Fig. 3 Schematic of the synthesis of 2D Porphyrin COFs (a) with tuneable content of fluoro-substituted monomer; reproduced from ref. 50. Copyright 2013, The American Chemical Society, and (b) with tuneable content of hydrogen-bonding structures; reproduced from ref. 51. Copyright 2015, The American Chemical Society.

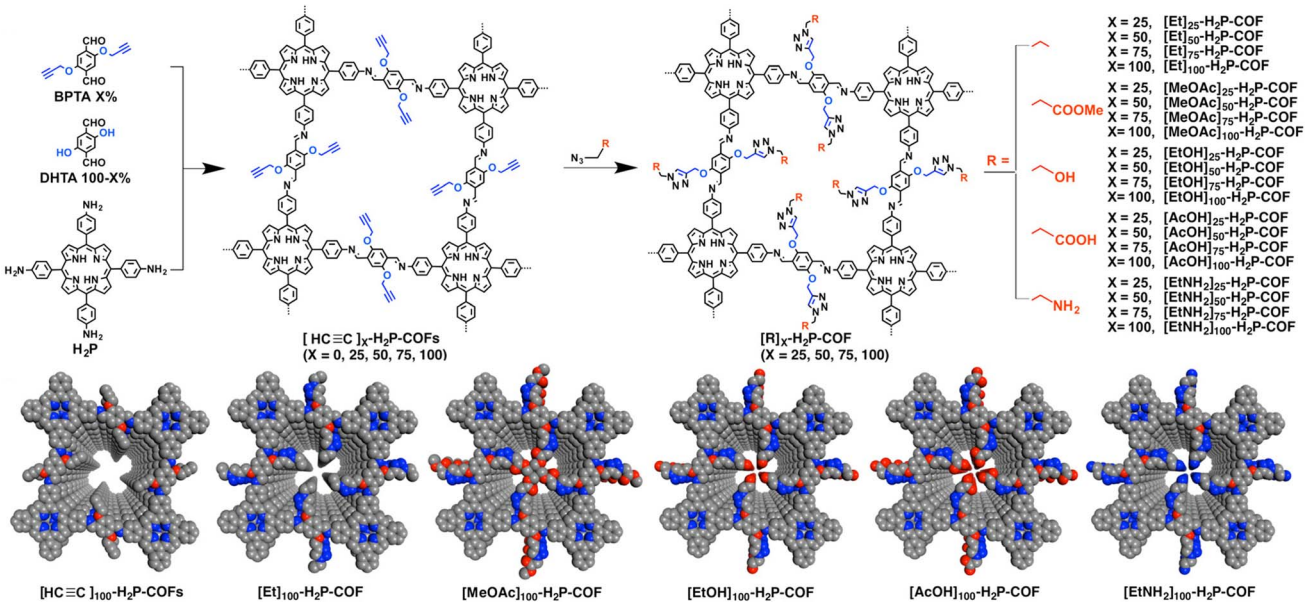

Fig. 4 Schematic of pore surface engineering of imine-linked COFs with various functional groups *via* click reactions and pore structures of COFs with different functional groups (Gray, C; Blue, N; Red, O); reproduced from ref. 53. Copyright 2015, The American Chemical Society.

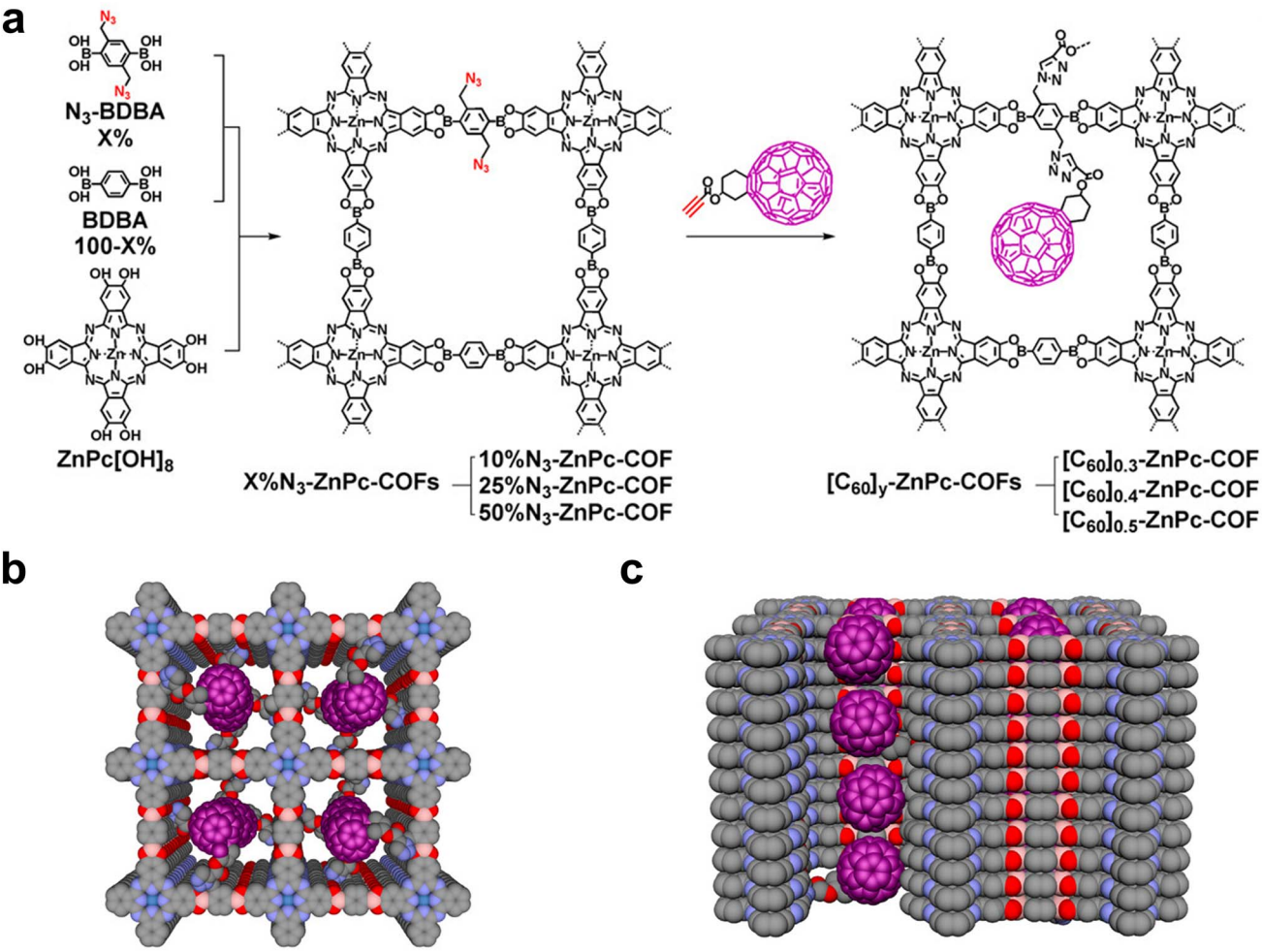

Fig. 5 (a) Schematic illustration of pore surface engineering of COFs incorporating C_{60} (depicted in purple); (b) top and (c) side views of a donor–acceptor COF with C_{60} integrated into the channel walls; reproduced from ref. 55. Copyright 2014, The American Chemical Society.

charge separation but also promote the formation of ordered heterojunctions. Under photoexcitation, these anisotropic and heterostructural frameworks facilitate efficient charge separation and stabilize long-lived radical intermediates. The extent of charge transfer is directly correlated with the fullerene loading, underscoring the critical role of tailored pore functionalization in optimizing photoelectric conversion. These results highlight how the strategic engineering of both skeleton anisotropy and pore geometry in MC-COFs can effectively modulate electronic structures and enhance photophysical performance.

Together, these innovations illustrate how isostructural mixed-monomer assembly and post-synthetic modification strategies offer powerful means to achieve gradient-level control over COFs functionality, paving the way for tailor-made porous materials in catalysis, ion transport, adsorption, and beyond.

3.2 Heterostructure mixed-monomer strategy

The heterostructure mixed-monomer strategy marks the beginning of the systematic study of MC-COFs. Addressing the limitations of conventional binary [1 + 1] condensation systems, typically constructed from one knot and one linker, Jiang and co-workers pioneered a generalizable approach based on [1 + 2] and [1 + 3] multicomponent condensation (Fig. 6).[57] This strategy enables the construction of crystalline hexagonal and tetragonal frameworks by integrating a single knot with two or three distinct linkers in one-pot copolymerization.

Unlike their binary counterparts, MC-COFs generated through this approach exhibit asymmetric assembly of molecular building blocks, giving rise to anisotropic skeletons and irregular pore shapes. Such structural complexity is inaccessible in traditional COFs and opens new avenues for spatially controlled functionality. Moreover, this synthetic platform proves especially powerful for D–A frameworks, allowing for the deliberate integration of multiple donor and acceptor linkers within the same lattice. The resulting electronic properties deviate significantly from the linear combination of individual components, demonstrating synergistic behaviours in charge delocalization, bandgap modulation, and photo-response. This multicomponent strategy not only expands the topological and compositional diversity of COFs but also introduces a versatile paradigm for precision tuning of framework architecture and function.

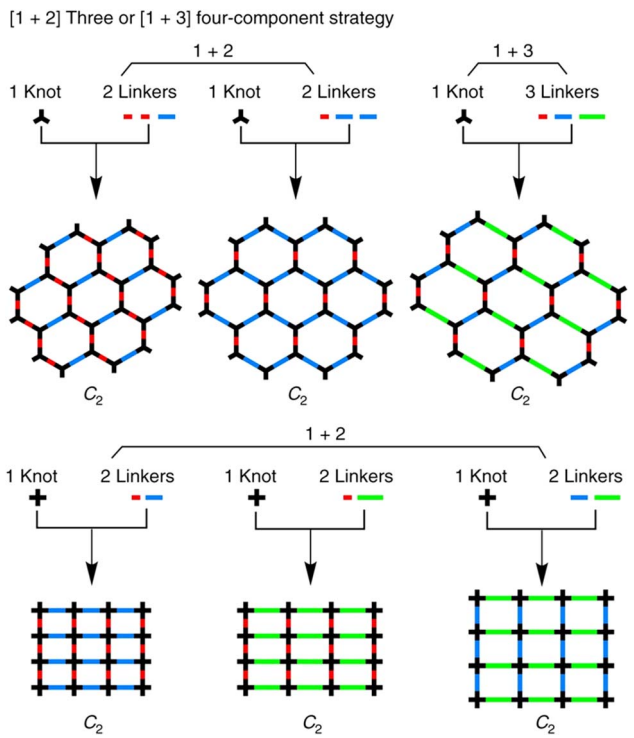

Fig. 6 Multiple-component [1 + 3] or [1 + 4] strategy for the synthesis of hexagonal and tetragonal MC-COFs. Three linkers shown in different colors and with different lengths are used to illustrate the typical knot-linker combinations in the MC strategy.

3.3 Multicomponent topological design

While traditional dual-component COFs predominantly adopt high-symmetry, edge-transitive topologies (Fig. 2a), their structural diversity is inherently constrained by the geometry and connectivity of binary component systems. In contrast, MC-COFs significantly broaden the design space by integrating building blocks with disparate geometries, connectivity, and symmetries. This multicomponent topological design enables the deliberate construction of complex, non-edge-transitive nets that remain inaccessible to single- or bi-component frameworks.

A representative example is COF-346, reported by Yaghi and co-workers, which integrates hexatopic, tetratopic, and tritopic linkers into a 2D framework with **tth** topology, characterised by three distinct types of vertices and two kinds of edges (Fig. 7).[28] The realization of this topology relied on precise geometric matching of linkers with angles of 60°, 90°, and 120°, and lengths around 7.1 Å, satisfying the closure requirements of quadrilateral rings within the net. The success of this design sets a benchmark in the reticular synthesis of non-edge-transitive COFs and demonstrates how controlled asymmetry can be harnessed to create highly intricate lattice motifs.

Concurrently, Lotsch *et al.* introduced a sub-stoichiometric design strategy to construct frameworks incorporating tri- and tetratopic units with deliberately unreacted sites (Fig. 8a).[58] For example, pyrene tetramine (P), nominally a tetradentate monomer, was combined in a 1 : 1 ratio with tritopic aldehydes (*e.g.*, triazine tribenzaldehyde or benzene tripicolinaldehyde). Only two of the four amine sites in P participated in bond formation, effectively rendering P a bidentate unit. These unreacted amines were later used to incorporate linear diamines, giving rise to frameworks with mixed bidentate–tridentate–tetradentate connectivity topological arrangements unattainable *via* conventional COFs strategies. In a complementary approach, Yaghi *et al.* demonstrated a hierarchical reticulation strategy, wherein pre-formed 1D COFs ribbons (COF-76) with pendant amines were further extended *via* imine or imide linkages to generate 2D frameworks (COF-77 and COF-78) exhibiting **bex** topology (Fig. 8b).[59] This stepwise or *in situ* linking of partially condensed intermediates exemplifies a powerful modular pathway to structural complexity.

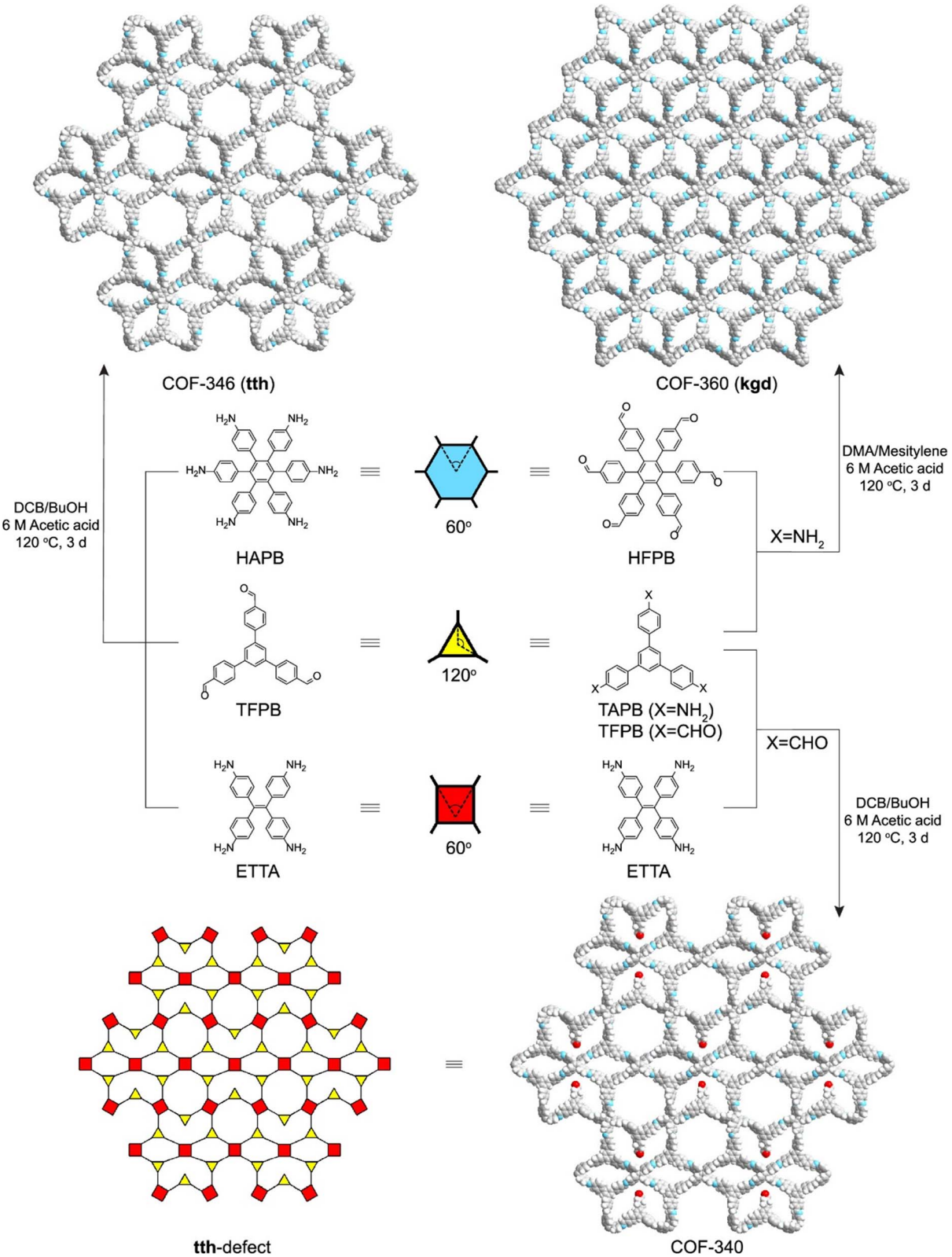

Fig. 7 Synthetic scheme for COF-346, -340, and -360. Color code: H, white; C, gray; N; blue; O, red. Frustrated aldehydes are randomly oriented in the COF-340 structure; reproduced from ref. 28. Copyright 2019, The American Chemical Society.

These strategies whether *via* frustrated functionalities, geometric asymmetry, or stepwise reticulation underscore the power of multicomponent topological design in transcending the limits of classical COFs topologies. Notably, the resulting frameworks retain high crystallinity and permanent porosity, confirming that complexity and order are not mutually

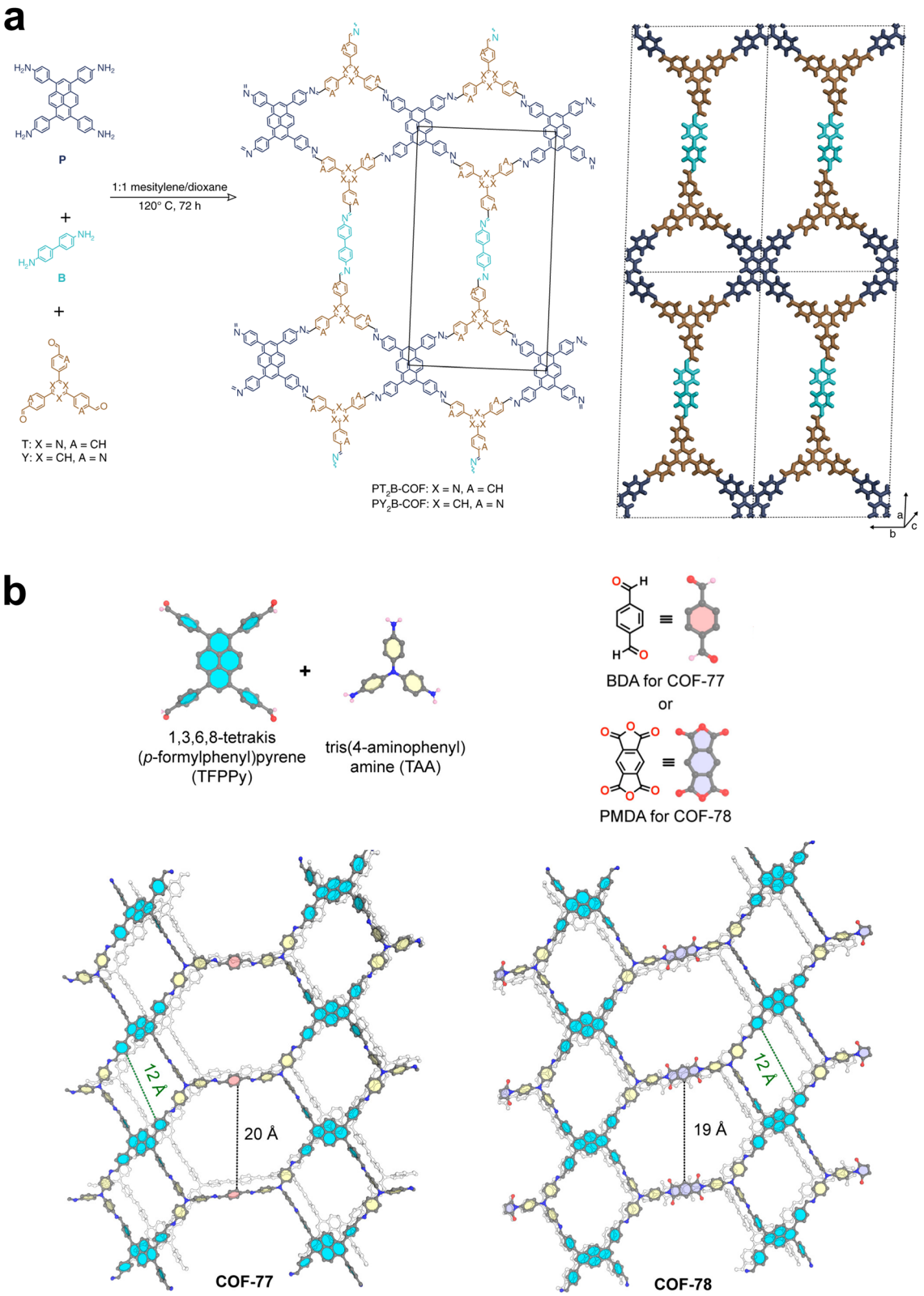

Fig. 8 (a) Structure of PT2B-COF and PY2B-COF. (b) Synthesis of COF-76 and COF-78. Atom sphere colors: C, gray; N, blue; O, red. Hydrogen atoms, except for aldehyde- and amine-hydrogens, omitted for clarity; reproduced from ref. 59. Copyright 2020, The American Chemical Society.

exclusive. Beyond structural novelty, this design paradigm enables the fine-tuning of pore architecture, spatial functionalization, and anisotropic properties, thus paving the way for highly programmable frameworks tailored for multisite catalysis, directional charge transport, and selective molecular recognition.

3.4 Multicomponent reactions

Multicomponent reactions (MCRs) in COF synthesis can be broadly classified into two categories. The first involves the use of hetero-functional linkers that undergo multiple condensation reactions in a one pot, thereby expanding the structural complexity of the resulting frameworks. A flagship example is 4-formylphenylboronic acid (FPBA), which was the first bifunctional linker shown to engage simultaneously in three reversible chemistries: (i) imine formation with amines, (ii) boronate ester formation with diols, and (iii) boroxine self-trimerization. Zhao *et al.* demonstrated this multireactive approach by combining FPBA with tris(4-aminophenyl) benzene (TAPB) to construct a hexagonal COF featuring boroxine rings and imine linkages in one pot.[60] When FPBA, TAPB and hexahydroxy triphenylene (HHTP) were mixed in a 3 : 1 : 1 ratio, the same system instead yielded a boronate-linked framework with concurrent imine connectivity. In both cases, the two reversible reactions

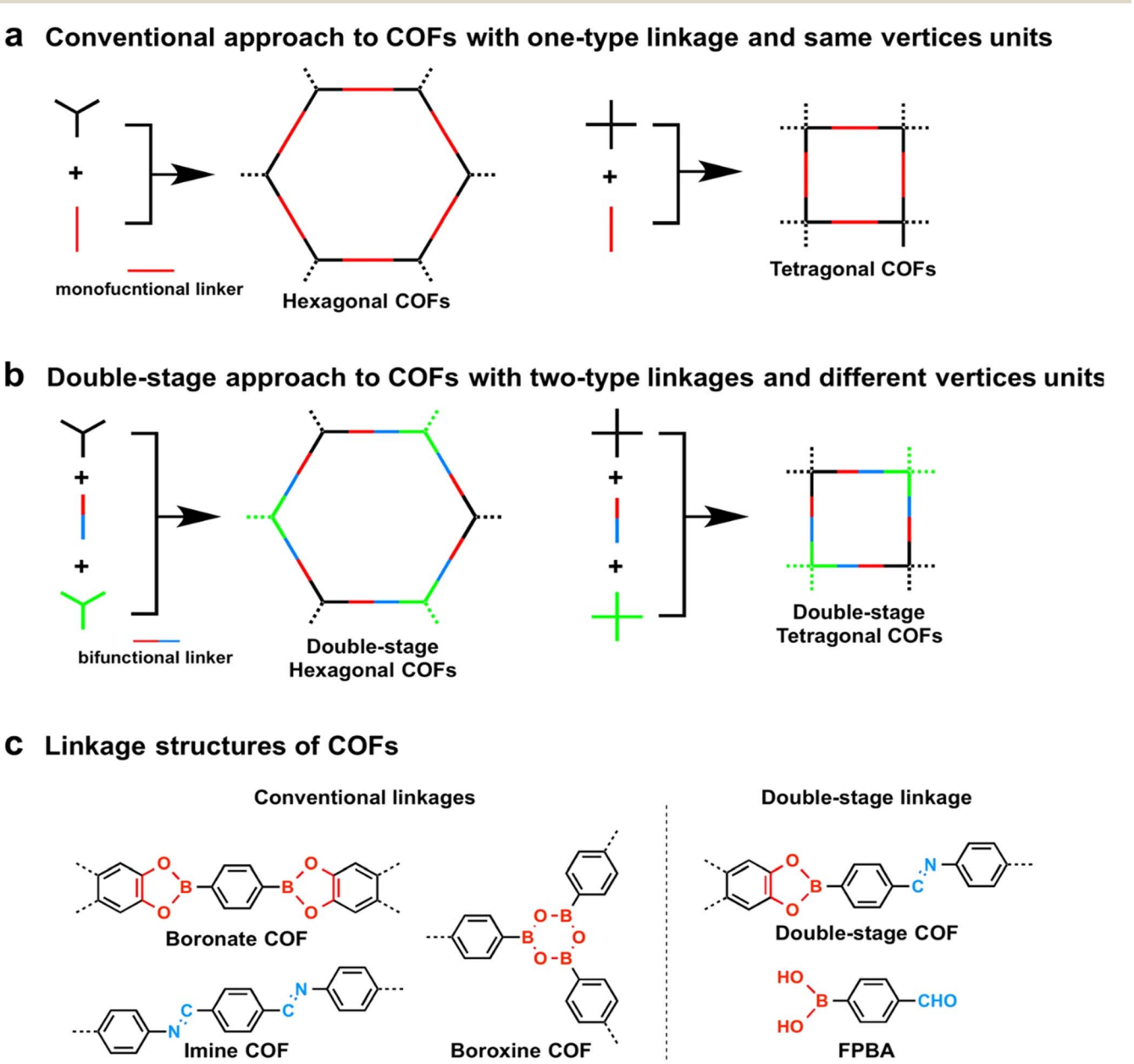

Fig. 9 (a) Schematic representation of the approaches to the conventional hexagonal and tetragonal COFs with monofunctional linkers made of two kinds of monomers. (b) Schematic representation of the double-stage approach to COFs with bifunctional linkers made of three different building blocks. (c) Typical linkage structures of boronate, boroxine and imine COFs and linkage structure of the double-stage COFs along with the structure of the bifunctional linker 4-formylphenylboronic acid (FPBA).

cooperated to drive error correction and crystallization, an outcome that eluded all stepwise synthetic attempts.

At the same time, Jiang *et al.* conducted an extensive investigation of FPBA-based multireactive COFs (Fig. 9a and b).[61] By pairing FPBA or substituted FPBAs with a variety of diamines, triamines and tetramines (to form imine bonds) and with tridentate or tetradentate polyhydroxyl ligands (to form boronate bonds), they synthesized twelve new COFs in one-pot reactions (Fig. 9c). Each framework was confirmed to be highly crystalline and porous, underscoring both the multifunctionality and generality of multireactive linker strategies for accessing novel architectures.

The second class comprises linkage-targeting multicomponent reactions, most commonly those based on imine condensations. In these schemes, three or more small building blocks are combined in a single reaction vessel to simultaneously forge the COF's linkage chemistry, an approach directly adapted from small-molecule MCRs, which are celebrated for their atom economy and rapid diversification of molecular skeletons (Fig. 10). When translated to COF synthesis, these MCR protocols not only retain such advantages but also enable the direct incorporation of additional functional moieties into the framework backbone. Over the past few years, this strategy has facilitated the rapid generation of a variety of robust COFs—featuring linkages such as quinolines,[62] thiazoles,[63] and imidazoles,[64] each exhibiting superior chemical stability and broadened functionality compared to their stepwise-assembled counterparts. A substantial body of work by Dong *et al.* has showcased the power of these MCRs,[65] and comprehensive reviews have already covered this topic in depth; accordingly, we do not expand further on linkage-targeting MCRs in this Perspective.

3.5 Pore portion strategy

As previously noted, most MC-COFs are synthesised *via* one-pot reactions. At the same time, PSM strategies for MC-COFs have been successfully employed to introduce structural complexity

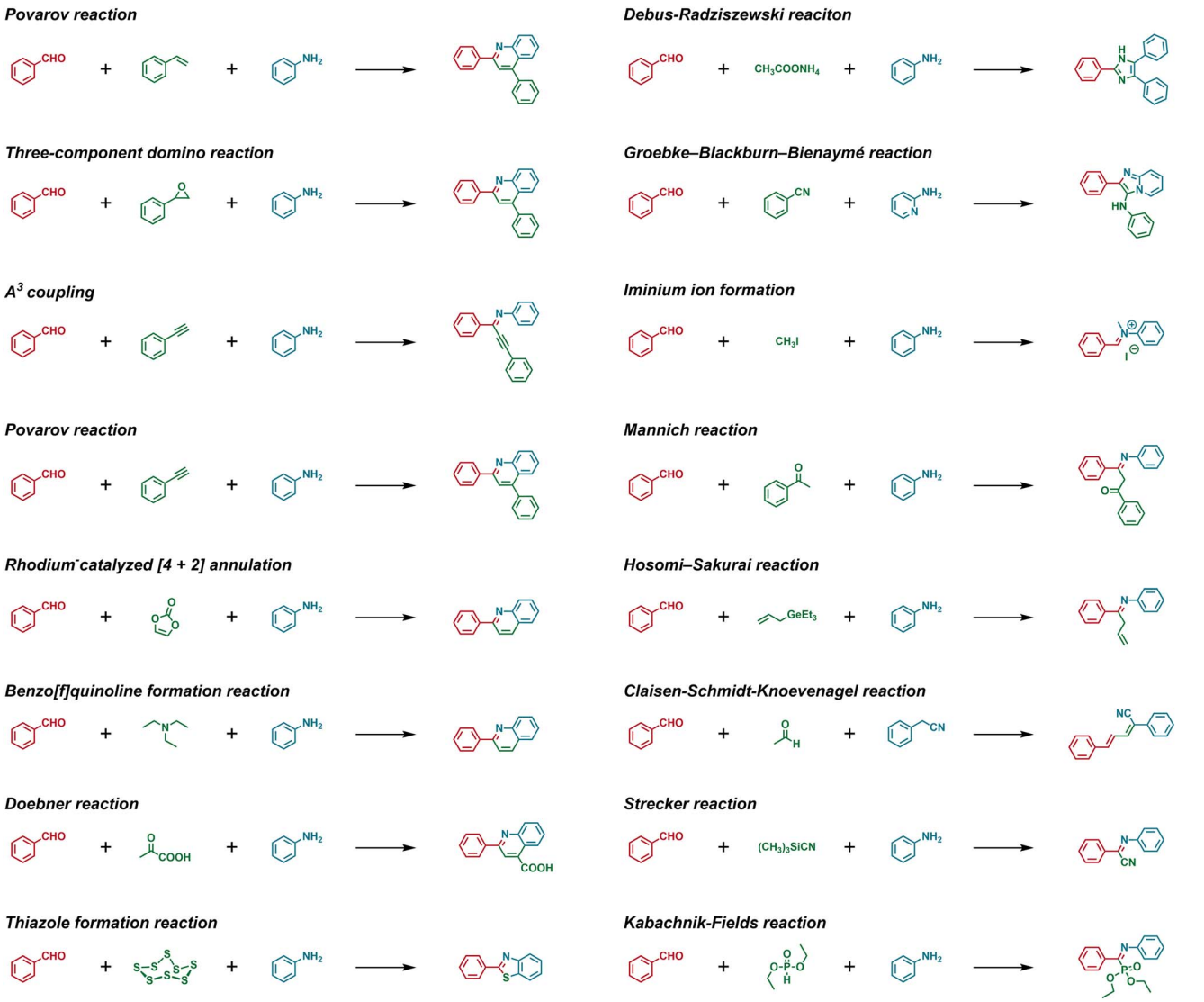

Fig. 10 Representative imine-based MCRs used for COFs construction.

and functional heterogeneity, but precise structural characterization and control remain limited. In particular, PSM approaches specifically aimed at modulating pore space and pore size have received comparatively little attention. Recent advances, however, highlight the promising potential of incorporating additional functional units into the COFs skeleton to partition internal pore space, pore portion strategy that offers a novel route toward the fine-tuning of pore dimensions and framework functionalities.

A representative and insightful example was reported by Huang *et al.*,[13] who employed a pore portion strategy to transform a mesoporous boroxine-linked COFs with an intrinsic pore diameter of 2.9 nm into six equivalent microporous domains, each with a uniform pore size of 6.5 Å (Fig. 11a and b). The key challenge in implementing such a partitioning strategy lies in achieving precise spatial control over the anchoring sites of the additional functional components within the framework channels. Typically, aldehyde or amine groups present along the channel walls serve as anchoring points, enabling the division of the pore space into smaller domains (*e.g.*, micropores or ultra-micropores). The feasibility of this strategy strongly depends on the geometric symmetry and size compatibility between the parent framework and the partitioning moieties. Achieving such structural complementarity is crucial for maintaining crystallinity and ensuring well-defined structure–property relationships. Furthermore, Wang *et al.* predesigned COFs pores by anchoring aldehyde groups at specific positions.[66] They then relied on this method to synthesise all-imine linked MC-COFs, subsequently inserting additional symmetric building blocks with C_2 or C_3 symmetry as pore dividers. This method enables tetragonal or hexagonal pores to be divided into two or three smaller micropores, respectively. It also demonstrates that the pore-splitting method exhibits a certain degree of ligand tolerance.

Overall, this strategy represents a significant advancement in the functional exploitation of COFs pore space, enabling the implementation of pre-designed compositions, components, and functionalities with unprecedented precision.

4 Applications of MC-COFs

Porous materials have demonstrated significant advantages across a wide range of applications. Among them, metal–organic frameworks benefit from a vast library of metal nodes and organic linkers, exhibiting high crystallinity and tuneable functionality, yet often face challenges in terms of stability under harsh conditions. In contrast, porous organic polymers offer remarkable synthetic versatility and robustness, but generally lack long-range structural order and crystallinity. COFs represent an emerging class of materials that combine

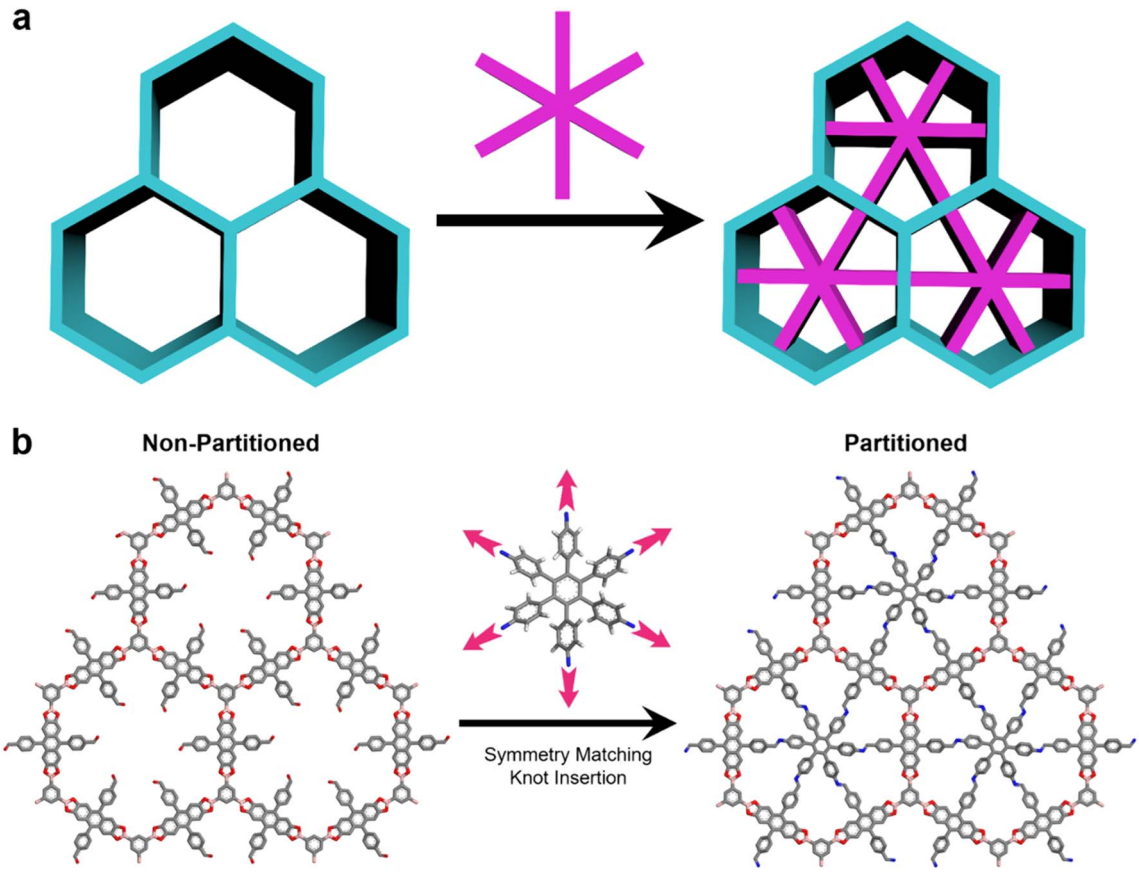

Fig. 11 (a) Graphical representation of pore partition in hexagonal channels. (b) Transformation of DBAAn-BTBA-COF into DBAAn-BTBA-HAPB-COF through symmetry matching knot insertion.

crystalline order with designable organic architectures, enabling precise exploration of advanced functionalities. Structurally, the properties of COFs can be systematically engineered at multiple levels: the molecular backbone, the pore environment, and their mutual interactions. This hierarchical structural control underpins the multifunctional performance of COFs.

Conventional single- or dual-component COFs have demonstrated structural regularity and well-defined porosity, but their functional scope is often constrained by limited compositional diversity. By integrating multiple components within a crystalline framework, MC-COFs combine the structural precision of COFs with the functional diversity of multivariate design, thereby enabling synergistic properties that are inaccessible to these related systems. Among them, MC-COFs offer an even higher degree of compositional and structural complexity, enabling the construction of intricately tailored pore environments and the precise modulation of electronic properties. However, a central challenge remains: to establish clear relationships between structural parameters and functional outputs, and to elucidate the fundamental mechanisms governing their emergent behaviours. In this section, we present recent advances in the functional design of MC-COFs, with a particular emphasis on structure–property relationships. We highlight their broad spectrum of applications, including electrocatalysis, photocatalysis, organocatalysis, gas adsorption and separation, wastewater remediation, luminescence, and radiotherapy, demonstrating how the deliberate integration of multiple components translates into enhanced and diversified performance profiles.

4.1 Electrocatalysis

COFs possess well-defined skeletons, tunable pore environments, and robust chemical stability, making them promising platforms for heterogeneous catalysis, including electrocatalysis, photocatalysis, asymmetric catalysis, and noble-metal-free catalysis. Their ordered nanochannels serve as confined nanoreactors, while the framework backbones offer programmable sites for catalytic function integration. Due to their insolubility in most solvents yet ability to form stable dispersions, COFs also facilitate multiphase catalysis with easy recovery and recyclability.

In the context of electrocatalysis, the introduction of multicomponent strategies to construct MC-COFs offers powerful means to finely regulate the electronic structure of the framework, especially through the rational arrangement of donor and acceptor moieties. While conventional D–A COFs typically incorporate a single pair of donor and acceptor units, this configuration often permits only broad, undirected modulation of intermediate binding strengths. In contrast, MC-COFs enable the integration of multiple, strategically positioned donor and acceptor segments, allowing precision-level control over charge localization, frontier orbital alignment, and active-site reactivity.

For instance, Long *et al.* reported a dimensionally graded MC-COF (TAE-COF) that alternates between 2D unsaturated and 3D saturated domains.[67] This hybrid structure introduced localised electronic disorder and pore-size heterogeneity, optimizing both mass transport and interfacial kinetics. The material exhibited a remarkable H_2O_2 production rate of 8.50 mol g_{cat}^{-1} h^{-1}, significantly surpassing its single-component counterparts. *In situ* ATR-FTIR and DFT simulations identified the central carbon atoms of the tetraphenyl motifs as catalytically active sites. Similarly, Wang *et al.* synthesised a fully conjugated 3D MC-COF (BUCT-COF-7) using an imidazole linkage *via* a one-pot Debus–Radziszewski multicomponent reaction.[68] The framework displayed excellent oxygen reduction reaction (ORR) performance, achieving 83.4% H_2O_2 selectivity and a production rate of 326.9 mmol g^{-1} h^{-1} at 10 mA cm^{-2}, owing to extended π-conjugation and heteroatom-enriched conduction pathways.

In other studies for carbon dioxide reduction reaction (CO_2RR), Zeng and co-workers reported a MC-COF constructed by integrating CoTAPP, PATA, and TAPZ units into a single framework (CoTAPP-PATA-TAPZ-COF).[69] This multicomponent design modulates intra-framework charge-transfer behavior, optimizing *COOH intermediate binding and *CO desorption during CO_2 electroreduction. As a result, the catalyst achieved a faradaic efficiency of 97.2% at −0.8 V *vs.* RHE and a current density of 27.85 mA cm^{-2} at −1.0 V, demonstrating both high selectivity and intrinsic activity. Furthermore, Zeng *et al.* demonstrated that boronic ester-linked MC-COFs can significantly enhance CO_2RR performance (Fig. 12a).[69] In this study, a multicomponent COFs was synthesised using 1,4-phenylenediboronic acid (PBBA) and Co-hexadecafluorophthalocyanine (TFPc), resulting in the formation of TFPc-PBBA-COF. This framework exhibited an impressive turnover frequency (TOF) of 1695.3 h^{-1} and a CO selectivity of 95.0% at −0.9 V, highlighting its high intrinsic activity and product specificity. The boron-based linkages not only facilitated the formation of *COOH intermediates but also played a crucial role in stabilizing the Co(II) active sites. To gain mechanistic insight into the catalytic process, *operando* X-ray absorption spectroscopy (XAS) was employed. In a potassium bicarbonate electrolyte saturated with carbon dioxide, XANES and EXAFS spectra at the cobalt K edge were recorded under the following sequential conditions: open-circuit potential (OCP), application of a −0.8 V bias (relative to the reduction potential), and return to OCP. Notably, no significant spectral shifts were observed throughout these transitions, suggesting that the oxidation state and coordination environment of Co(II) remained stable during CO_2 adsorption, reduction, and CO desorption. This spectral invariance indicates a robust catalytic centre and enabled the authors to propose a detailed mechanistic model involving CO_2 activation and the structural evolution of the Co-site during electrochemical CO_2RR (Fig. 12b). This research endeavor serves as a testament to the significant structural benefits that these MC-COFs offer in the context of CO_2 reduction reactions.

In the context of nitrate electroreduction (NO_3RR), Cheng *et al.* introduced a multivariate COFs strategy to engineer the interfacial microenvironment *via* controlled electrostatic potential (ESP) modulation (Fig. 13a).[70] By co-polymerizing ethidium

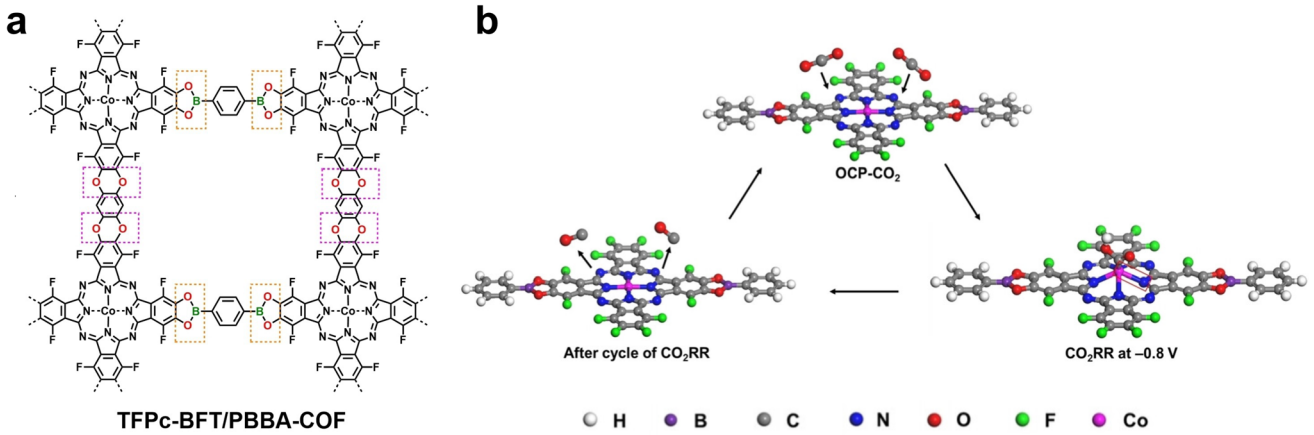

Fig. 12 (a) Chemical structure of TFPc-BFT/PBBA-COF. (b) Schematic illustration for activation processes of TFPc-BFT/PBBA-COF. Reproduced from ref. 69. Copyright 2024, Wiley-VCH.

bromide (EB) and benzidine (BD) as linkers, they synthesised a boronic ester-based MC-COF (BECOF) with tunable ESP properties. The optimised BECOF-modified catalyst exhibited an ammonia yield of 11.01 mmol h^{-1} mg^{-1} and a faradaic efficiency of 91.0%, outperforming the pristine PdCu electrode. Mechanistic investigations revealed that in acidic electrolyte, the surface of the bare electrocatalyst is dominated by an excess of protons, while the diffusion of nitrate ions is relatively inefficient, resulting in significant competition from the hydrogen evolution reaction (HER). Upon deposition of a near-neutral BECOF adlayer, interfacial proton diffusion was partially suppressed *via* physical sieving, while nitrate ions were simultaneously enriched through weak electrostatic attraction. This enrichment effect increased the local NO_3^-/H^+ ratio, thereby favoring selective NO_3^--to-NH_3 conversion (Fig. 13b). Crucially, a volcano-type trend in NO_3RR performance was observed as a function of BECOF thickness. Increasing the coating from 0.5BECOF/PdCu to BECOF/PdCu improved ammonia yield, whereas excessive loading (2BECOF/PdCu) led to diminished performance due to over-shielding of the active interface. These findings underscore the delicate balance required to modulate ion transport: while an optimal positive ESP promotes selective nitrate reduction,

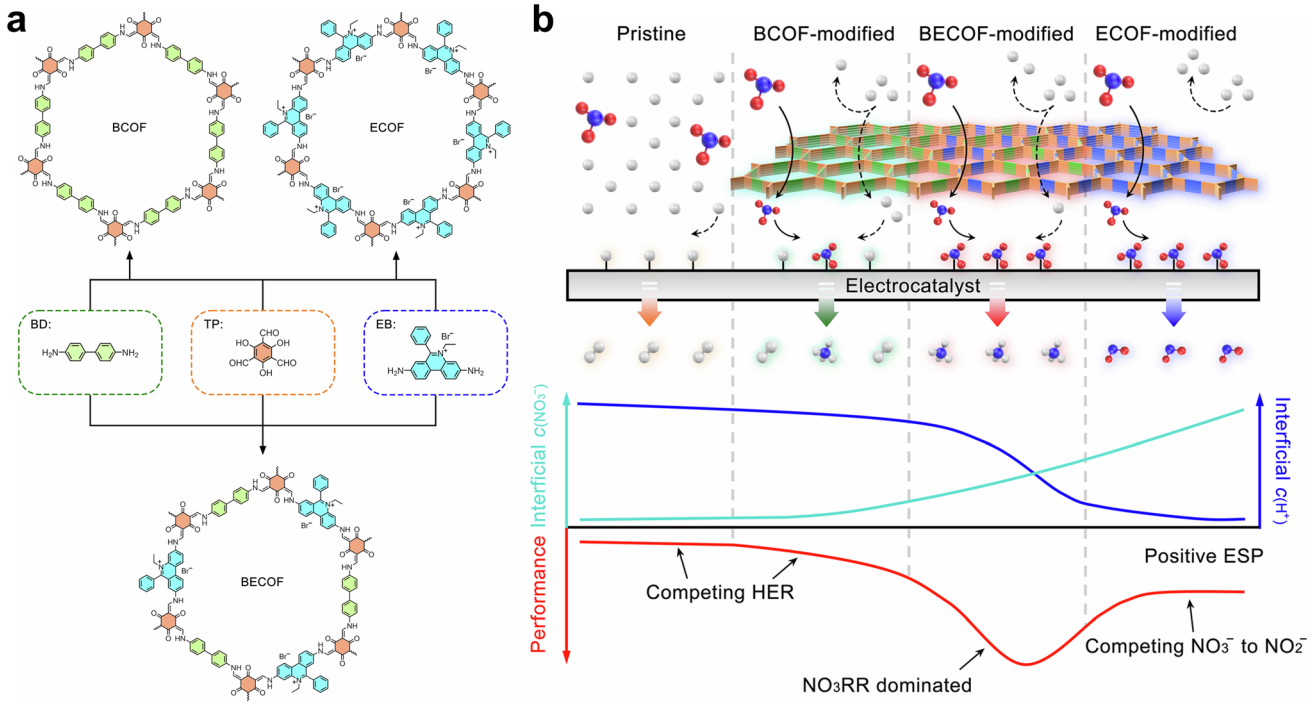

Fig. 13 (a) Synthetic scheme of multivariate COFs. Aromatic rings are coloured to assist in the differentiation of the origin of the different moieties (orange, 2,4,6-triformylphloroglucinol, TP; green, benzidine, BD; azure, ethidium bromide, EB). (b) Schematic illustration for improving NO_3RR performance by using multivariate COFs with tailored ESP. COFs are coloured to assist in the differentiation of the origins of the different moieties (orange vertices, TPs; green linkers, BDs; blue linkers, EBs). Blue spheres, N; red spheres, O; white spheres, H.

excessive electrostatic bias may impede proton availability and hinder hydrogenation steps. Notably, BECOF outperformed ECOF, a structurally similar COFs with even higher ESP, indicating that maximizing NO_3^-/H^+ ratios is not always advantageous, and rational tuning of local charge environments is essential for catalytic optimization.

These collective advancements underscore the versatility of MC-COFs in electrocatalysis. Through compositional and structural engineering, MC-COFs enable precise control of charge transfer, intermediate stabilization, and electronic configuration. Future research will likely emphasise understanding structure–performance relationships and expanding synthetic methodologies to access increasingly complex and functional MC-COF electrocatalysts.

4.2 Photocatalysis

Compared with electrocatalysis, photocatalysis imposes more stringent requirements on the orchestration of electronic

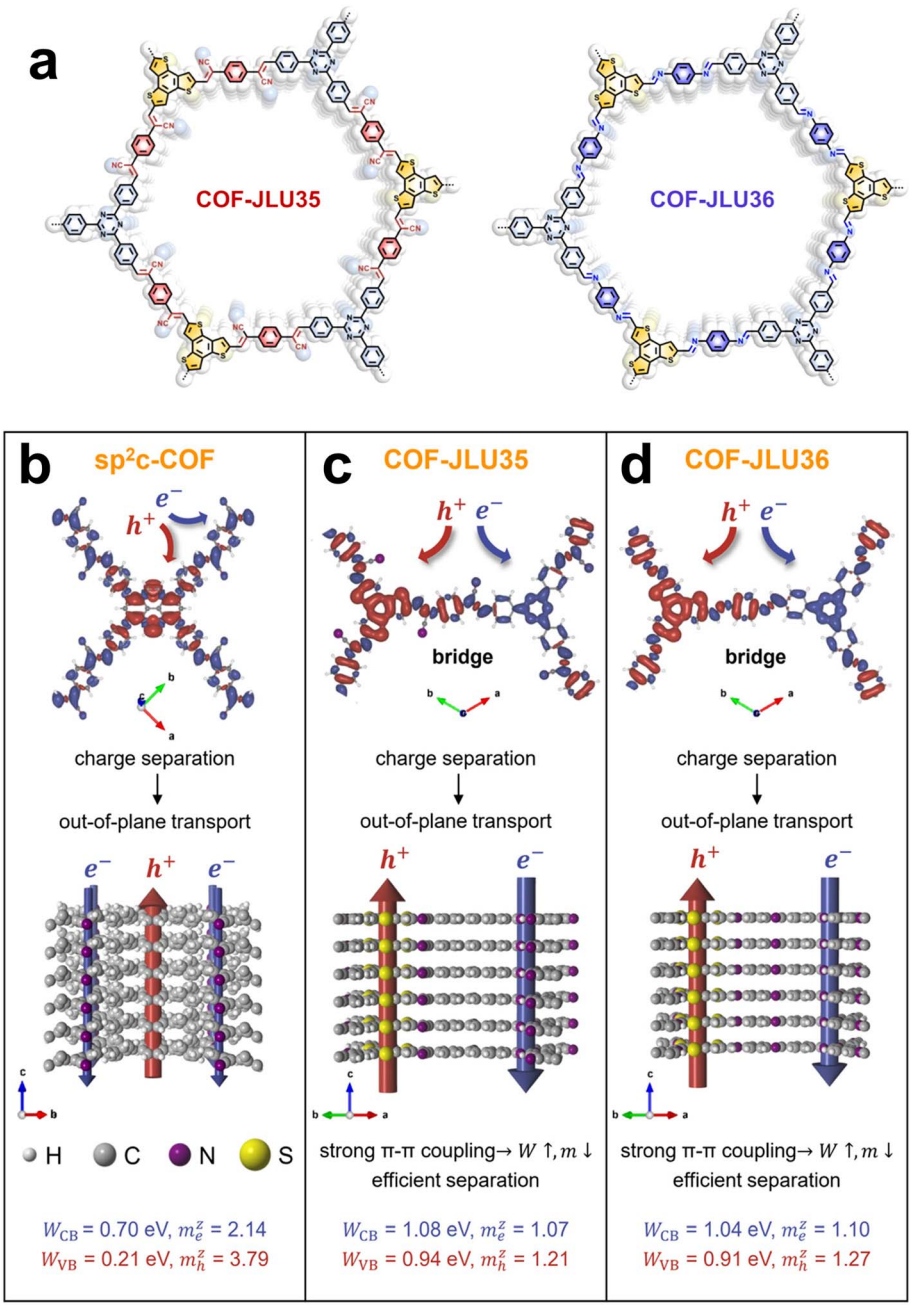

Fig. 14 (a) Chemical structure of COF-JLU35 and COF-JLU36; Top view of charge separation (upper panel) and the side view of charge transport channels (lower panel) are schematically shown for (b) sp^2c-COF, (c) COF-JLU35, and (d) COF-JLU36. The positive (red) and negative (blue) isosurfaces of HOMO–LUMO density difference ($\rho_{HOMO} - \rho_{LUMO}$) indicate different locations of electron and hole centres. The conduction bandwidth (WCB), valence bandwidth (WVB), cross-planar electron mass, and hole effective mass are given at the bottom. Reproduced from ref. 23. Copyright 2023, The American Chemical Society.

structures, including precise alignment of valence and conduction band edges, efficient suppression of charge recombination, and optimised exciton dynamics. Owing to their modularity and extended π-conjugation, MC-COFs offer a versatile platform for band-structure engineering *via* the synergistic incorporation of multiple π-bridges, donors, and acceptors.

Guo *et al.* demonstrated that adjusting the monomer feed ratio in MC-COFs enables fine modulation of the optical bandgap and energy levels, thus improving both light-harvesting capacity and redox potentials to enhance photocatalytic hydrogen evolution.[21] Liu *et al.* constructed a donor–π–acceptor-type COFs (COF-JLU35) by integrating electron-deficient triazine and electron-rich benzothieno[3,2-*b*]thiophene units through sp^2 carbon and imine linkages (Fig. 14a).[23] Both DFT calculations and photoelectrochemical experiments confirmed that this tricomponent architecture promoted exciton dissociation and accelerated charge carrier mobility, achieving a hydrogen evolution rate of 70.8 ± 1.9 mmol g^{-1} h^{-1} under visible light, outperforming many state-of-the-art COF-based photocatalysts. Further theoretical analysis revealed that the donor–π–acceptor motifs in COF-JLU35 and its analogue COF-JLU36 enabled spatial HOMO–LUMO separation, which is more pronounced than in two-component COFs like sp^2c-COF (Fig. 14b). In COF-JLU35, full π-conjugation reduced the in-plane electron effective mass ($1.63m_e$ *vs.* $4.70m_e$ in COF-JLU36), enhancing lateral charge mobility. Bader charge analysis showed that acceptor TFPT units are more positively charged in COF-JLU35, thereby favoring electron migration and interlayer delocalization. These features collectively contribute to more efficient charge separation and reduced recombination, consistent with observed photocatalytic performance.

In parallel, Thomas and co-workers synthesized quinoline-4-carboxylic acid-linked MC-COFs (DMCR-COFs) *via* a one-pot Doebner multicomponent reaction.[71] By systematically varying the conjugation length and linker substitution patterns, they tailored the photoelectronic properties to significantly boost H_2O_2 production. Notably, DMCR-COF-1NH operated efficiently in pure water without sacrificial agents while maintaining structural integrity across a wide pH range. Expanding this strategy, the same group developed a family of donor–acceptor-type quinoline-linked COFs (PCOF-1 to PCOF-5) *via* the Povarov reaction.[72] By varying vinyl-functionalized monomers, they introduced diverse pore chemistries, with the imidazole-containing PCOF-4 exhibiting the highest crystallinity, surface area, and hydrophilicity—yielding optimal hydrogen evolution performance.

In a related study, Dong *et al.* developed benzo[f]quinoline-linked MC-COFs through a three-component [4 + 2] cyclo-condensation (Fig. 15a).[73] These frameworks exhibited high crystallinity, thermal stability, and broadband visible-light absorption. Mechanistic investigations showed that H_2O_2 was simultaneously produced *via* dual pathways: the ORR and the water oxidation reaction (WOR). Upon visible-light excitation, photogenerated electrons drove the ORR to form H_2O_2 from O_2, while holes on the valence band participated in WOR to oxidize water, also producing H_2O_2 (Fig. 15b). The optimized system achieved an exceptional H_2O_2 generation rate of 9025 μmol g^{-1} h^{-1} in pure water without any sacrificial agents, outperforming most COF-based benchmarks.

These studies collectively highlight the power of multicomponent engineering in enabling rational control over exciton dynamics, orbital alignment, and redox functionality. Looking ahead, the integration of gradient conjugation, adaptive pore environments, and redox-active linkages into MC-COFs offers promising routes toward next-generation solar-driven systems. A key future direction lies in coupling MC-COF design with *operando* spectroscopies and machine learning to reveal structure–function relationships at the molecular level, paving the way for predictive design of efficient, robust, and scalable photocatalysts tailored for solar fuel production and green oxidative transformations.

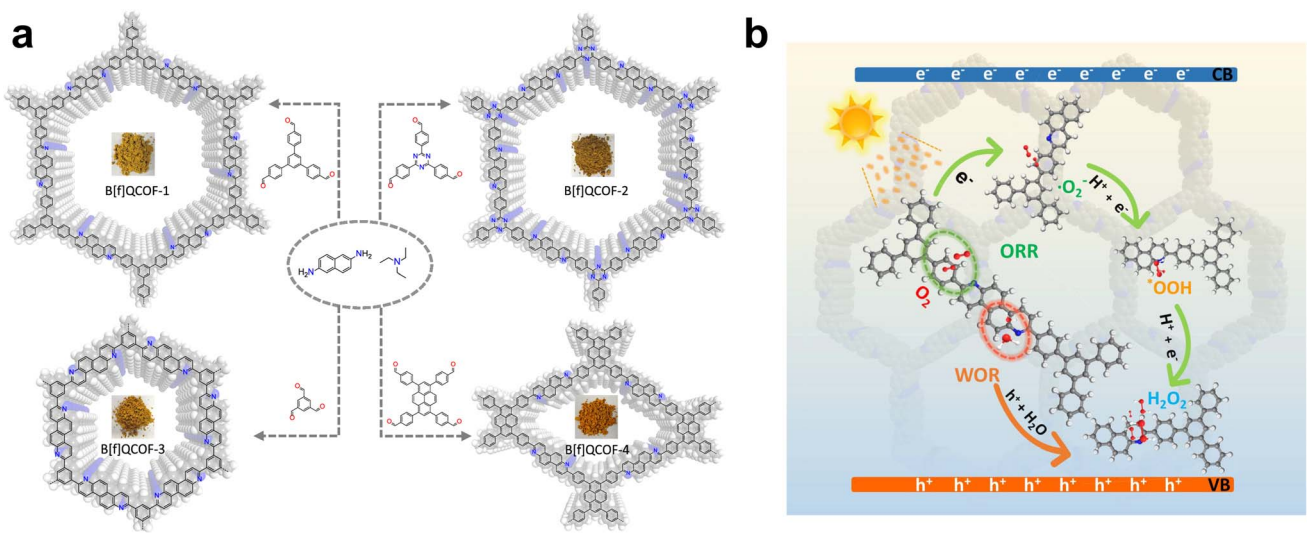

Fig. 15 (a) Synthesis of the benzo[f]quinoline-linked COFs *via* one-pot three-component [4 + 2] cyclic condensation. (b) The proposed mechanism diagram for the photocatalytic synthesis of H_2O_2 over the B[f]QCOFs *via* both ORR and WOR pathways.

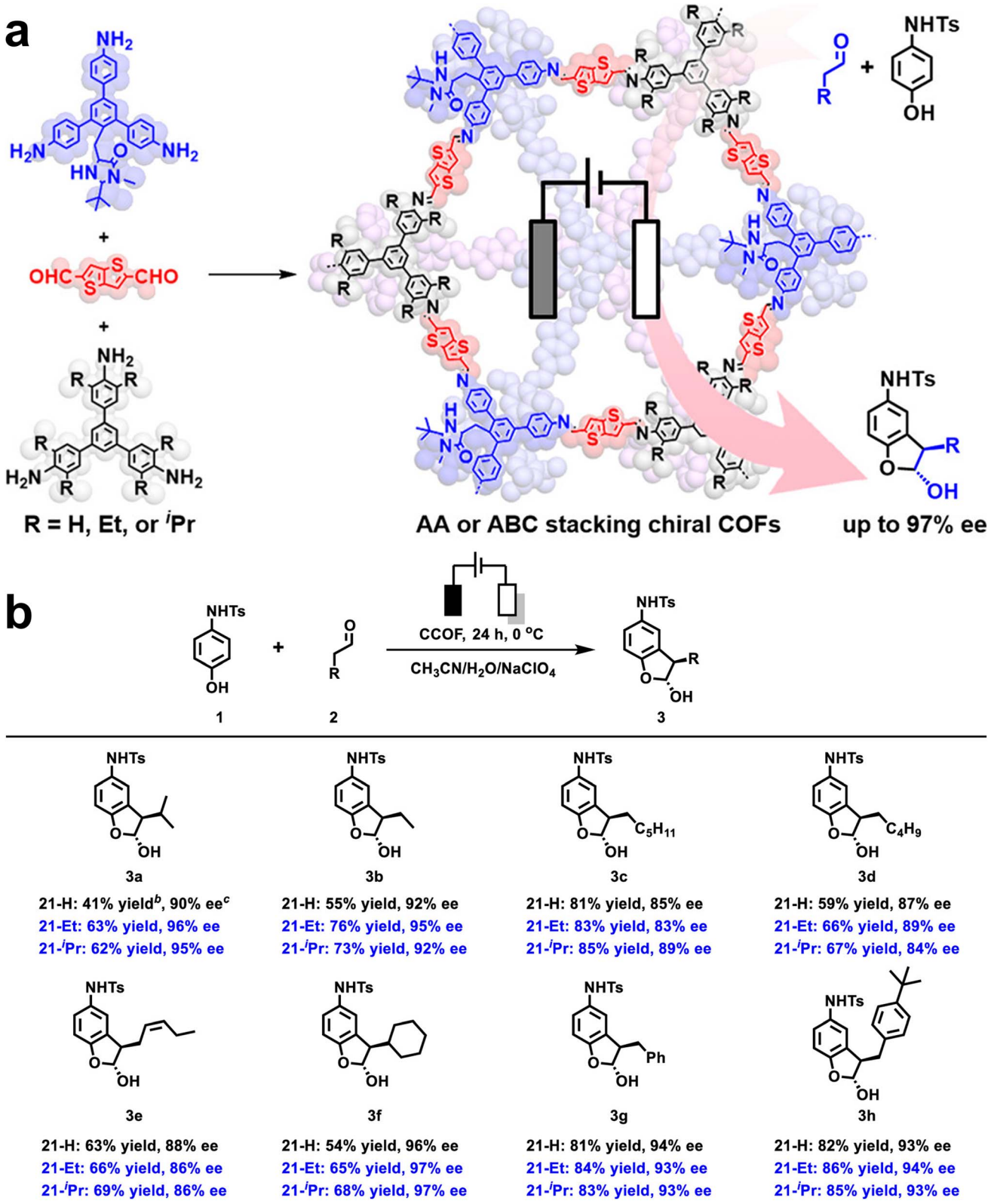

Fig. 16 (a) Synthesis of the mixed-linker COFs for electrochemical asymmetric catalysis yields and (b) ee values of the electrochemically induced asymmetric α-arylation of aldehydes; reproduced from ref. 74. Copyright 2023, The American Chemical Society.

4.3 Organocatalysis

In addition to their electrocatalytic and photocatalytic capabilities, MC-COFs have shown considerable promise in the realm of organocatalysis. Their modular design, high structural fidelity, and capacity to spatially integrate multiple functional moieties afford well-defined reaction microenvironments

that enable synergistic modulation of both reactivity and selectivity.

A notable example is the chiral 2D MC-COFs developed by Cui *et al.*, featuring tunable interlayer stacking modes (Fig. 16a).[74] By varying the monomer feed ratio, the stacking configuration could be altered from AA to ABC, significantly impacting the electronic properties of the framework. The ABC-stacked variant demonstrated superior enantioselective electrocatalytic performance in the asymmetric α-arylation of aldehydes, achieving up to 97% enantiomeric excess (ee) *via* a coupled anodic oxidation/organocatalysis strategy (Fig. 16b). Enhanced charge transport in the ABC-stacked configuration was identified as the key factor underpinning its improved selectivity and activity.

In a complementary approach, Xiang *et al.* synthesised unsubstituted quinoline-bridged COFs (NQ-COFs) *via* a multicomponent reaction platform.[22] The resulting frameworks exhibited high crystallinity, large surface areas, and efficient superoxide ($O_2^{\bullet-}$) charge transfer channels, owing to the presence of electron-deficient quinoline linkages. These structural features facilitated selective oxidative coupling reactions under visible-light irradiation, exemplified by the synthesis of 2-substituted benzimidazoles, mediated by $O_2^{\bullet-}$ under visible-light irradiation. Further expanding the scope of organocatalytic MC-COFs, Lei *et al.* constructed a highly crystalline four-component COFs (DBTH4-COF) using HTB, TTB, BD, and DMBZ monomers *via* a solvothermal route.[75] This framework achieved high photocatalytic efficiency for benzimidazole synthesis under blue light (yield up to 91%), while maintaining structural integrity and activity over multiple cycles. Mechanistic investigations, including EPR analysis and control experiments, revealed the cooperative involvement of both singlet oxygen ($^1O_2$) and $O_2^{\bullet-}$, highlighting the complexity and versatility of the photochemical pathways. DBTH4-COF also catalysed the oxidation of benzylamines to imines (96% yield) and the transformation of tetrahydroisoquinolines to lactams (86% conversion), confirming its broad substrate scope and robustness.

In another innovative approach, Zhao *et al.* developed quinoline-linked COFs *via in situ* transformation of imine linkages using a one-pot Povarov reaction (Fig. 17a).[76] This synthetic strategy significantly enhanced the chemical stability of the COFs and enabled efficient photocatalysis under harsh conditions. The resulting materials exhibited excellent activity in oxidative decarboxylation and benzylamine coupling reactions, along with outstanding recyclability (Fig. 17b). Meanwhile, Traxler *et al.* introduced a multifunctional MC-COF system by incorporating both acridine and 2,2′-bipyridine units into the same framework.[77] This design endowed the material with broad-spectrum light absorption and accessible coordination sites for nickel catalysts, enabling its application as a heterogeneous metallaphotocatalyst for visible-light-driven carbon–heteroatom cross-coupling reactions.

These studies collectively demonstrate the rich potential of MC-COFs in organocatalytic transformations. The ability to co-integrate chiral centres, redox-active sites, and electron-transport motifs within a single periodic scaffold opens unprecedented avenues for fine-tuning catalytic selectivity and reactivity. Moving forward, the rational design of MC-COFs for cascade catalysis, asymmetric photocatalysis, and stimuli-responsive reactivity represents a fertile ground for innovation in molecular synthesis and sustainable chemistry.

4.4 Adsorption and separation

The efficient separation of alkane isomers remains an enduring challenge due to their chemical inertness and similar polarizabilities, leaving molecular shape as the primary distinguishing feature. For instance, the compound hexane, with the molecular formula C_6H_{14}, has five distinct isomers. These isomers exhibit considerable differences in their research octane number (RON), which is a crucial parameter that indicates a fuel's resistance to knocking. The RON values for these isomers are as follows: *n*-hexane (30), 2-methylpentane (74), 3-methylpentane (75), 2,3-dimethylbutane (105), and 2,2-dimethylbutane (94), each comprising 10–30% of commercial mixtures (Fig. 18a). To increase the RON of gasoline, zeolites have traditionally been used as molecular sieves to separate these isomers based on subtle steric differences, typically yielding RON values around 83.

COFs present a new frontier for shape-selective separation due to their highly tunable and crystalline pore architectures. Huang *et al.* adopted the pore partitioning strategy to develop a multicomponent COFs (DBAAn-BTBA-HAPB-COF) with uniform ultramicroporous channels (~0.65 nm) and wedge pore geometry (Fig. 18b–d).[13] This work provides a robust synthetic blueprint for constructing crystalline frameworks with hierarchically confined domains and represents the first example of COFs for the molecular sieving of hexane isomers. Because alkane isomers are chemically inert and possess closely matched physical properties, their effective separation has long been challenging. DBAAn-BTBA-HAPB-COF overcomes this obstacle by exploiting subtle differences in steric fit and van der Waals forces within its ultra-micropores. Pure-component adsorption isotherms reveal distinct uptakes across the five C_6 isomers, while dynamic breakthrough experiments, corroborated by molecular dynamics simulations, confirm its ability to selectively enrich branched isomers. The net result is the isolation of a hexane mixture with a research octane number (RON) exceeding 99, highlighting the material's practical impact for fuel upgrading.

This study marks a significant milestone in precision gas separation and highlights the emerging role of MC-COFs in hydrocarbon refinement. The integration of spatially defined ultra-micropores *via* multicomponent design not only enables tailored host–guest interactions but also establishes a paradigm for energy-efficient molecular sieving. Future directions may include dynamic pore modulation, incorporation of responsive functionalities, and process integration in continuous-flow fuel purification technologies.

4.5 Others

Beyond above application, MC-COFs, especially those containing metal centres or π-conjugated chromophores, have

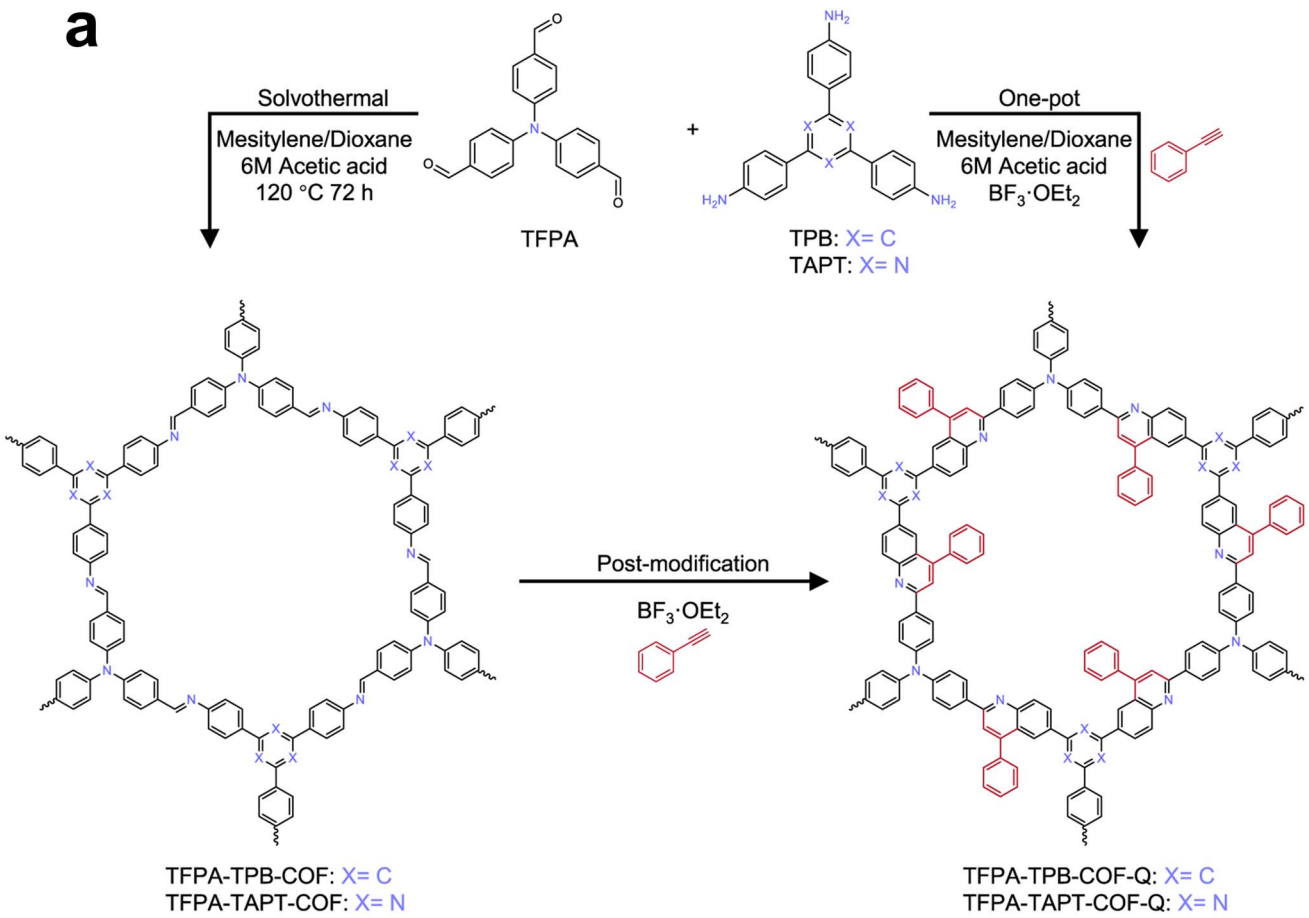

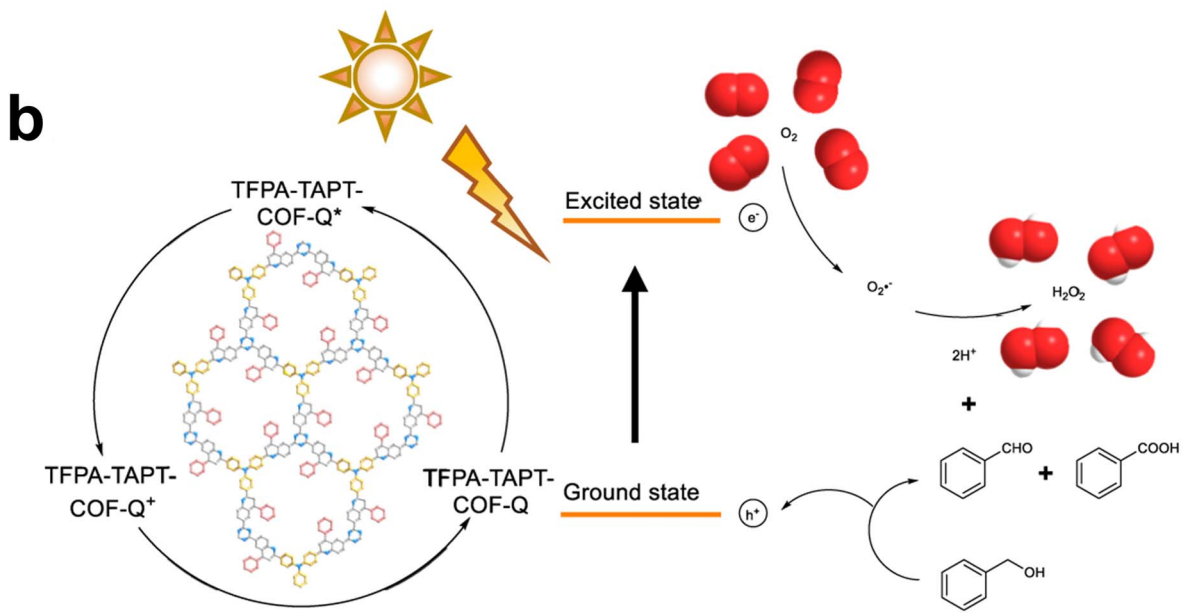

Fig. 17 (a) Synthesis of quinoline-linked COFs using a one-pot Povarov reaction. (b) Proposed mechanism for photocatalytic production of H_2O_2 using TFPA-TAPT-COF-Q as catalyst.

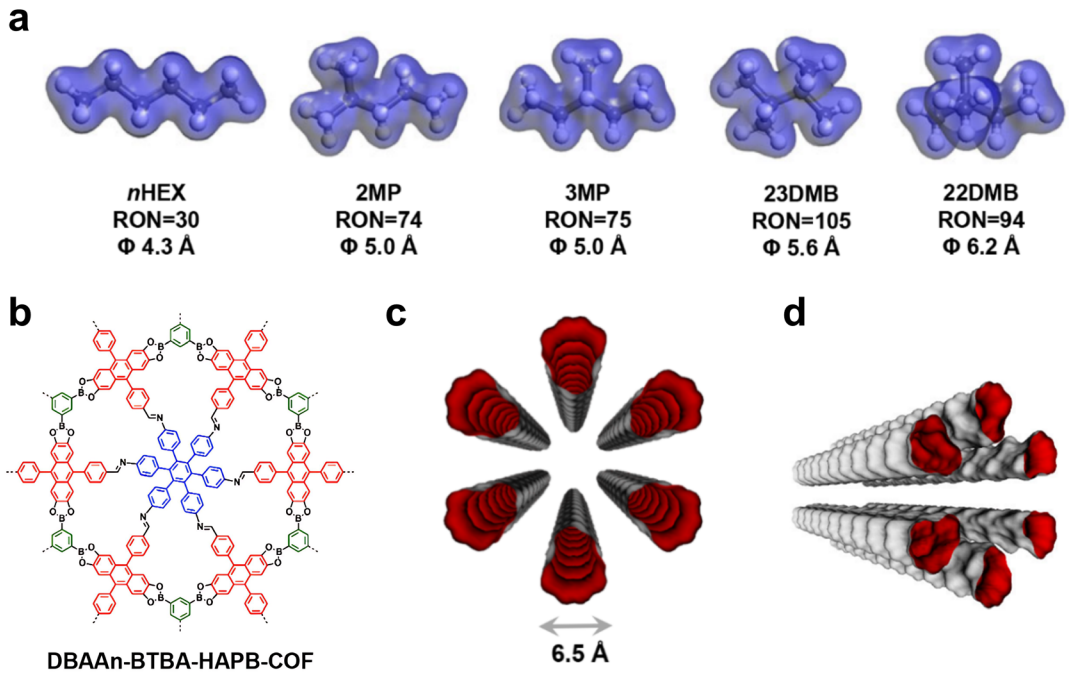

Fig. 18 (a) Hexane isomers (*n*HEX, 2MP, 3MP, 23DMB, and 22DMB) with their RONs and Φ values. Structural formula of (b) DBAAn-BTBA-HAPB-COF. (c) Top-view and (d) side-view van der Waals surfaces associated with the 1D channels running through DBAAn-BTBA-HAPB-COF.

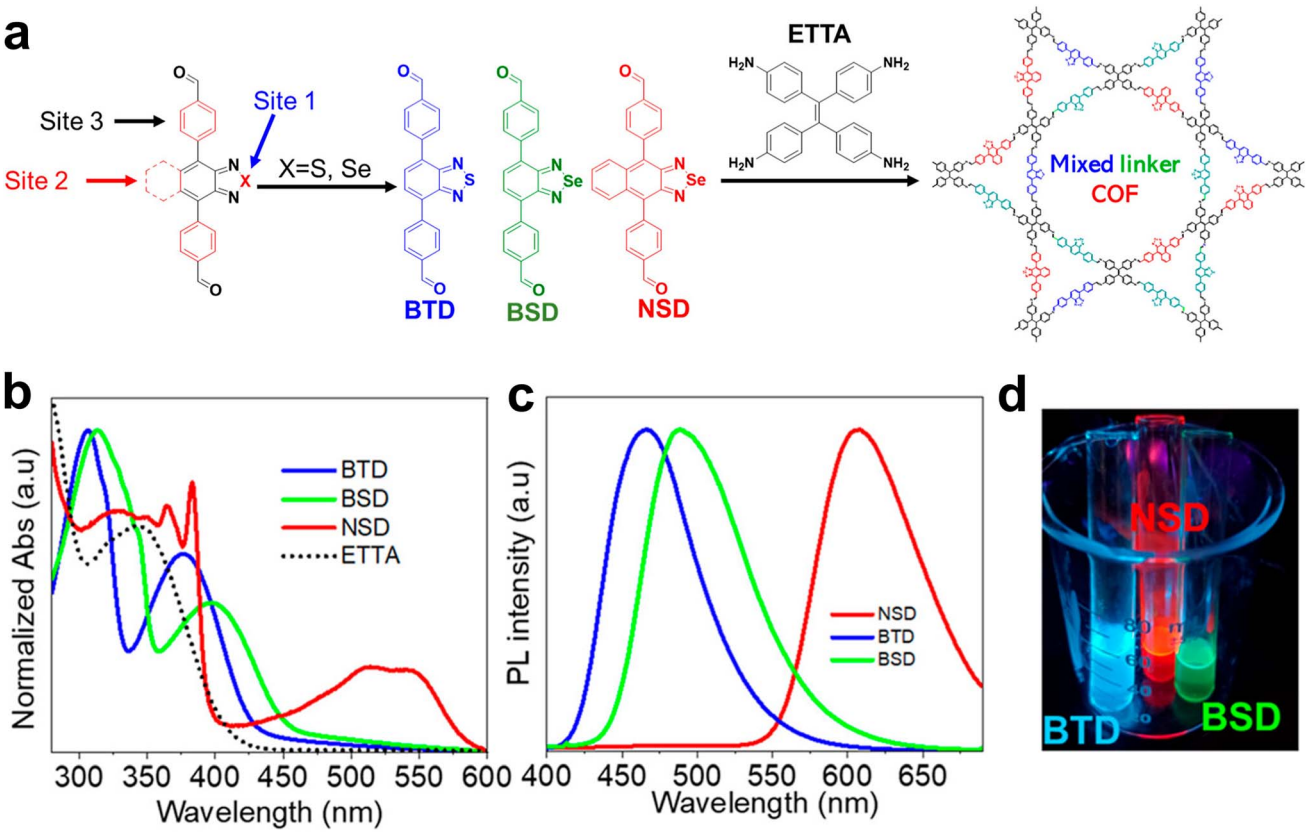

Fig. 19 (a) Chemical structure of mixed linker COF. (b) UV-visible absorption and (c) emission spectra of BTD, BSD, and NSD ligands in DCM at 365 nm excitation; (d) ligand emission under a 365 nm UV lamp. The absorption and emission spectra were scaled to facilitate a better comparison; reproduced from ref. 24. Copyright 2024, The American Chemical Society.

demonstrated outstanding performance across a wide range of emerging applications. Owing to their structural modularity and electronic tunability, MC-COFs are particularly suitable for developing functional materials in light-emitting, sensing, environmental remediation, and biomedical radiation.

In the field of optoelectronics, MC-COFs allow for precise control over energy transfer and emission behavior. Song *et al.* synthesised a series of TFPT[*X*]-BMTH-COFs exhibiting tunable intramolecular charge transfer (ICT) and aggregation-induced emission (AIE) properties by adjusting the molar ratio of the TFPT monomer.[26] Among them, TFPT[67]-BMTH-COF showed an ultralow water detection limit of 0.00007 wt%, and was successfully applied in the visual detection of trace water in honey and salt *via* fluorescent test strips, demonstrating the potential of MC-COFs for practical sensing applications. This precise spatial organization enables MC-COFs to serve as high-performance fluorescent sensors.

Huang *et al.* reported the construction of a white-light-emitting COFs through the co-integration of three emissive building blocks—BTD (blue), BSD (green), and NSD (red)—into

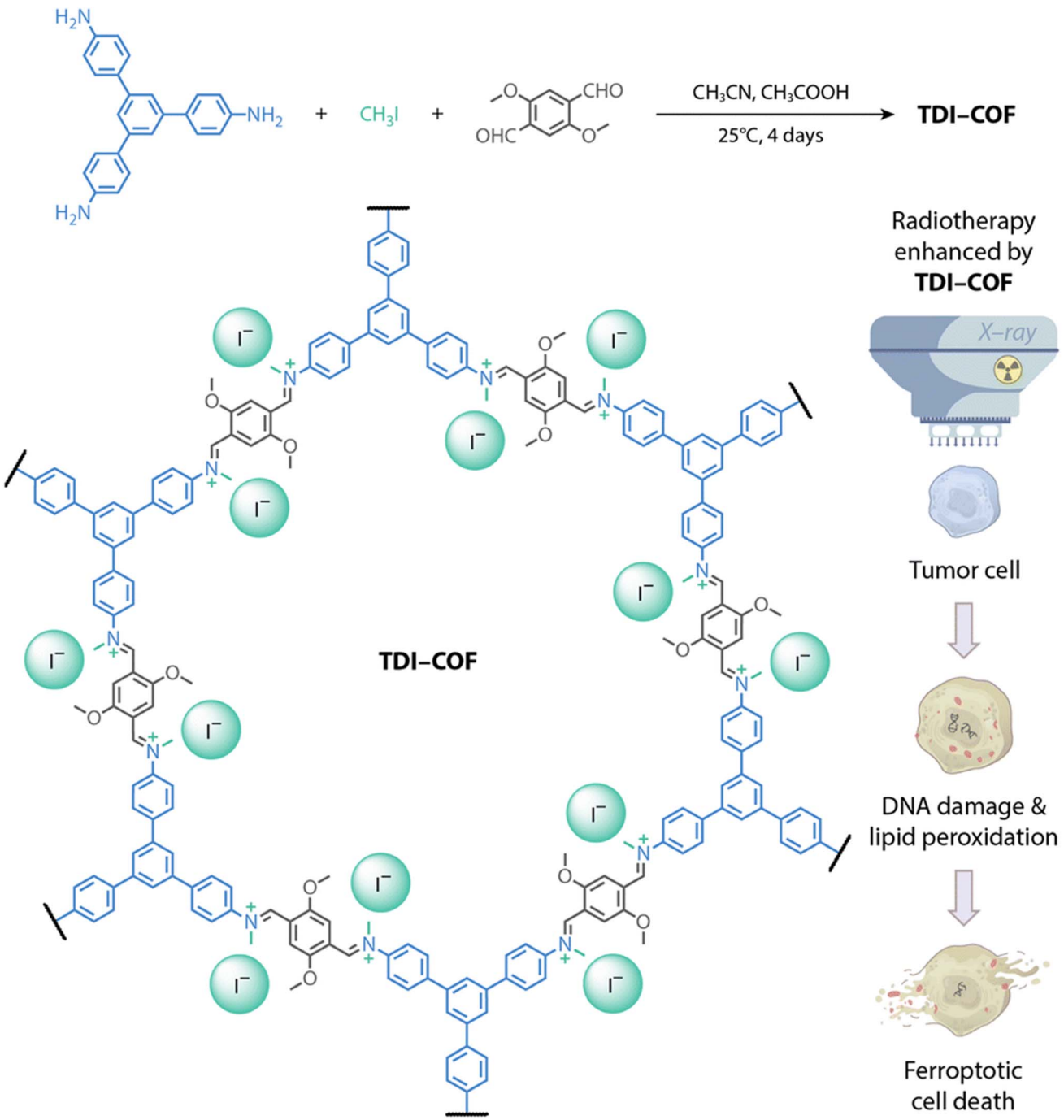

Fig. 20 Synthesis of an iodide-containing and iminium-linked TDI-COF as a radiosensitiser for improving radiotherapy efficacy *via* iodide-promoted X-ray deposition.

a single crystalline framework(Fig. 19a).[24] Efficient full-spectrum white-light emission was achieved exclusively when all three chromophores were spatially confined within the same MC-COF, enabling controlled cascade energy transfer from BTD to BSD and NSD. In contrast, physical mixtures of the free ligands or their respective single-ligand COFs failed to generate comparable emission profiles. UV-visible absorption (Fig. 19b) and emission spectra (Fig. 19c) of the three ligands, where exchanging S for Se (site 1) in BTD to form BSD results in the red-shifts of the absorption and emission by 20 and 22 nm, respectively. Increasing the conjugation by inserting a phenyl ring at the central benzoselenadiazole unit (site 2) in BSD to form NSD led to a significant red shift of both absorption and emission (~120 nm). The emission peaks appear at 466, 488, and 608 nm for BTD, BSD, and NSD (Fig. 19c), respectively, which correspond to the blue, green, and red regions of the visible spectrum under 365 nm excitation (Fig. 19d). This study exemplifies how multicomponent design facilitates chromophore co-localization, achieving complex photonic behavior that is inaccessible to mono-component systems.

In the realm of environmental analysis, MC-COFs also offer unique advantages for the enrichment and detection of persistent organic pollutants (POPs) in complex aqueous matrices. Liao *et al.* designed a fluorinated hydroxyl-functionalised COFs (OH-F-COF) *via* multicomponent assembly, incorporating multiple interaction motifs, including fluorophilicity, π–π stacking, hydrogen bonding, and electrostatic attraction.[25] This multifunctional framework demonstrated high-efficiency simultaneous enrichment of diverse pollutants such as perfluoroalkyl substances (PFAS), bisphenol A (BPA), and polychlorinated biphenyls (PCBs). Coupled with solid-phase extraction (SESE-SPE) and chromatographic techniques (HPLC-MS/MS and GC-MS), OH-F-COF enabled ultra-trace detection of these analytes, addressing longstanding analytical challenges in food and water safety.

In biomedical applications, MC-COFs are emerging as promising platforms for multifunctional therapy. Dong *et al.* developed a cationic, iodine-rich COFs (TDI-COF) through a one-pot three-component reaction, imparting radiosensitizing functionality (Fig. 20).[78] This MC-COF significantly enhanced the efficacy of radiotherapy by facilitating DNA double-strand breaks and lipid peroxidation, ultimately promoting ferroptosis-mediated tumor cell death. *In vivo* experiments confirmed effective suppression of colorectal tumor growth, demonstrating that rational integration of therapeutic components within an MC-COF scaffold can yield potent, multimodal therapeutic outcomes.

These studies collectively highlight the transformative potential of multicomponent design in expanding the functional landscape of COFs beyond catalysis. By enabling the co-localization of diverse chemical functionalities and fostering tunable intermolecular interactions, MC-COFs unlock unprecedented opportunities in light emitting, molecular recognition, environmental sensing, and targeted therapy. Looking forward, future efforts are expected to explore stimuli-responsive MC-COFs, spatiotemporal modulation of function, and bio-integrated hybrid systems, paving the way for intelligent materials that bridge molecular design and practical performance.

5 Conclusion and perspective

The rational construction of MC-COFs rests on three pillars: (i) deliberate topology design to accommodate building blocks of diverse symmetry and dimension within one crystalline network; (ii) the synthesis of tailored organic monomers, engineering for length, functionality, symmetry and solubility, that precisely match the chosen topology; and (iii) the fine-tuning of reaction parameters to orchestrate reversible covalent bonding, error correction and high-quality framework crystallization.

In this perspective, we have summarised recent advances in MC-COF synthesis, categorizing them into five overarching strategies: (1) isostructural mixed-monomer assemblies, which copolymerise linkers of identical connectivity but varied substitution patterns; (2) heterostructural mixed-monomer frameworks, which exploit asymmetric tiling and anisotropic pore geometries *via* [1 + 2] and [1 + 3] condensation schemes; (3) multicomponent topological design, which construct new topological diagrams of COFs using multicomponent monomers. (4) Multicomponent reactions, wherein three or more orthogonal dynamic covalent chemistries are combined in a single pot; and (5) pore partitioning, which splits large channels into uniform ultra-microporous domains by PSM insertion of symmetric partitioners. These approaches have yielded hundreds of new COFs, however, only a fraction of the conceivable combinations within the broader COF universe. Notably, some MC-COFs exhibit exceptional functions, from highly active photocatalysts to enantioselective electrocatalysts, owing to their complex periodic skeletons and hierarchically tailored pore environments. We foresee many opportunities in the design and synthesis of new COFs with multiple building blocks and in the exploration of new functions from multicomponent synergistic systems.

Despite these significant progresses, several critical challenges remain. First, the most challenging aspect in the field of MC-COFs is thorough characterization. Although direct synthetic routes are preferred, controlling the structural arrangement of the products is often quite difficult because a variety of arrangements can be produced in this way. In most literature reports, there is little detailed characterization of structural arrangements. The development of single crystals of MC-COFs is a challenging but still promising direction in COF chemistry. It is particularly necessary to elucidate the interactions between different incorporated components to better understand the interatomic interactions on larger length scales. Second, the repertoire of reversible and irreversible bond chemistries in MC-COFs remains narrow. Expanding beyond imine, boronate and boroxine linkages to include triazine, imide, amide, benzoxazole and other robust moieties will contribute to enrich MC-COFs in terms of species and regulatory properties. Careful balancing of linker flexibility, reaction kinetics, stacking interactions and bond reversibility will be essential to achieve high crystallinity in these more complex systems. Third, the true power of MC-COFs lies in synergistic

effects among co-integrated units, properties that cannot be accessed in single-component analogues. Realizing this potential will require predictive computational models and AI-driven design tools that can forecast structure–property relationships and guide the selection of monomer combinations optimized for target applications. Looking forward, the fusion of advanced computational modeling, AI-assisted inverse design and innovative synthetic methodologies promises to elevate MC-COF chemistry to a new level. By uniting precise topology engineering, monomer innovation and mechanistic insight, the next generation of MC-COFs will deliver bespoke porous materials tailored for advanced applications. Finally, several challenges remain for the practical deployment of MC-COFs in industrial settings. Key issues include the scalability of synthesis, the long-term structural stability under harsh operating conditions, and the relatively high cost of certain precursors. Addressing these limitations will be essential to bridge the gap between laboratory research and real-world applications.

Author contributions

X. X. and N. H. performed the literature search, analyzed the published results, and wrote the manuscript.

Conflicts of interest

The authors declare no competing financial interest.

Data availability

As a comprehensive review of existing published research, all discussed data and findings are derived from previously reported studies.

Acknowledgements

This work is supported by financial support from the National Key R&D Program of China (2022YFE0130700), the National Natural Science Foundation of China (22375173) and Postdoctoral Fellowship Program of CPSF under Grant Number GZB20250042.

Notes and references

1 C. S. Diercks and O. M. Yaghi, *Science*, 2017, **355**, eaal1585.
2 K. T. Tan, S. Ghosh, Z. Wang, F. Wen, D. Rodríguez-San-Miguel, J. Feng, N. Huang, W. Wang, F. Zamora, X. Feng, A. Thomas and D. Jiang, *Nat. Rev. Methods Primers*, 2023, **3**, 1.
3 S.-Y. Ding and W. Wang, *Chem. Soc. Rev.*, 2013, **42**, 548–568.
4 A. P. Côté, A. I. Benin, N. W. Ockwig, M. O'Keeffe, A. J. Matzger and O. M. Yaghi, *Science*, 2005, **310**, 1166–1170.
5 K. Geng, T. He, R. Liu, S. Dalapati, K. T. Tan, Z. Li, S. Tao, Y. Gong, Q. Jiang and D. Jiang, *Chem. Rev.*, 2020, **120**, 8814–8933.
6 N. Huang, P. Wang and D. Jiang, *Nat. Rev. Mater.*, 2016, **1**, 16068.
7 R. Liu, K. T. Tan, Y. Gong, Y. Chen, Z. Li, S. Xie, T. He, Z. Lu, H. Yang and D. Jiang, *Chem. Soc. Rev.*, 2021, **50**, 120–242.
8 X. Xu, Y. Feng, H. Chen and N. Huang, *J. Am. Chem. Soc.*, 2025, **147**, 16653–16660.
9 S. Paul, M. Gupta, A. Kumar Mahato, S. Karak, A. Basak, S. Datta and R. Banerjee, *J. Am. Chem. Soc.*, 2024, **146**, 858–867.
10 N. Huang, K. H. Lee, Y. Yue, X. Xu, S. Irle, Q. Jiang and D. Jiang, *Angew. Chem., Int. Ed.*, 2020, **59**, 16587–16593.
11 X. Xu, Q. Cui, H. Chen and N. Huang, *J. Am. Chem. Soc.*, 2023, **145**, 24202–24209.
12 F. Jin, E. Lin, T. Wang, S. Geng, T. Wang, W. Liu, F. Xiong, Z. Wang, Y. Chen, P. Cheng and Z. Zhang, *J. Am. Chem. Soc.*, 2022, **144**, 5643–5652.
13 X. Xu, X. Wu, K. Xu, H. Xu, H. Chen and N. Huang, *Nat. Commun.*, 2023, **14**, 3360.
14 Y. Xu, J. Gong, Q. Li, X. Guo, X. Wan, L. Xu and H. Pang, *Nanoscale*, 2024, **16**, 11429–11456.
15 Y. Wang, Q. Hao, Q. Lv, X. Shang, M. Wu and Z. Li, *Chem. Commun.*, 2024, **60**, 10046–10063.
16 X. Xu, S. Zhang, K. Xu, H. Chen, X. Fan and N. Huang, *J. Am. Chem. Soc.*, 2023, **145**, 1022–1030.
17 N. Keller and T. Bein, *Chem. Soc. Rev.*, 2021, **50**, 1813–1845.
18 X. Xu, S. Wang, Y. Yue and N. Huang, *ACS Appl. Mater. Interfaces*, 2020, **12**, 37427–37434.
19 L. Ascherl, E. W. Evans, J. Gorman, S. Orsborne, D. Bessinger, T. Bein, R. H. Friend and F. Auras, *J. Am. Chem. Soc.*, 2019, **141**, 15693–15699.
20 X. Zheng, W. Qiu, J. Cui, H. Liu, Y. Zhao, J. Zhang, Z. Zhang and Y. Zhao, *Chem.–Eur. J.*, 2024, **30**, e202303004.
21 T. Zhou, X. Huang, Z. Mi, Y. Zhu, R. Wang, C. Wang and J. Guo, *Polym. Chem.*, 2021, **12**, 3250–3256.
22 H. Pang, D. Huang, Y. Zhu, X. Zhao and Y. Xiang, *Chem. Sci.*, 2023, **14**, 1543–1550.
23 Z. Li, T. Deng, S. Ma, Z. Zhang, G. Wu, J. Wang, Q. Li, H. Xia, S.-W. Yang and X. Liu, *J. Am. Chem. Soc.*, 2023, **145**, 8364–8374.
24 J. Nyakuchena, H. Chiromo, S. Radpour, J. Guckenburg and J. Huang, *ACS Appl. Mater. Interfaces*, 2024, **16**, 44921–44926.
25 J. Gong, Y. Chen, W. A., X. Zhang, J. Ma, Z. Xie, P. Li, A. Huang, S. Zhang and Q. Liao, *J. Hazard. Mater.*, 2024, **472**, 134563.
26 L. Zou, M. Li, X. Wang, M. Ye, L. Chen, L. Wang and Y. Song, *Spectrochim. Acta, Part A*, 2024, **311**, 123978.
27 C. Qian and X. Zhao, *Acc. Chem. Res.*, 2025, **58**, 1192–1209.
28 B. Zhang, H. Mao, R. Matheu, J. A. Reimer, S. A. Alshmimri, S. Alshihri and O. M. Yaghi, *J. Am. Chem. Soc.*, 2019, **141**, 11420–11424.
29 S. Wang, X. Xu, Y. Yue, K. Yu, Q. Shui, N. Huang and H. Chen, *Small Struct.*, 2020, **1**, 2000021.
30 J.-R. Wang, K. Song, T.-X. Luan, K. Cheng, Q. Wang, Y. Wang, W. W. Yu, P.-Z. Li and Y. Zhao, *Nat. Commun.*, 2024, **15**, 1267.
31 Y. Luo, Y. Qin, C. Ni, C. Liu, H. Yan, Y. Tao, W. Du and J. Zou, *Chem. Eng. J.*, 2024, **497**, 154941.
32 A. F. M. EL-Mahdy, C.-H. Kuo, A. Alshehri, C. Young, Y. Yamauchi, J. Kim and S.-W. Kuo, *J. Mater. Chem. A*, 2018, **6**, 19532–19541.

33 J. M. Rotter, R. Guntermann, M. Auth, A. Mähringer, A. Sperlich, V. Dyakonov, D. D. Medina and T. Bein, *Chem. Sci.*, 2020, **11**, 12843–12853.
34 D. Li, C. Li, L. Zhang, H. Li, L. Zhu, D. Yang, Q. Fang, S. Qiu and X. Yao, *J. Am. Chem. Soc.*, 2020, **142**, 8104–8108.
35 H. Wei, J. Ning, X. Cao, X. Li and L. Hao, *J. Am. Chem. Soc.*, 2018, **140**, 11618–11622.
36 L. Gilmanova, V. Bon, L. Shupletsov, D. Pohl, M. Rauche, E. Brunner and S. Kaskel, *J. Am. Chem. Soc.*, 2021, **143**, 18368–18373.
37 S. Feng, H. Xu, C. Zhang, Y. Chen, J. Zeng, D. Jiang and J.-X. Jiang, *Chem. Commun.*, 2017, **53**, 11334–11337.
38 C. Wang, W. Lu, W. Song, Z. Zhang, C. Xie, Y. Li and J. Wang, *Appl. Catal. B Environ. Energy*, 2025, **361**, 124583.
39 C.-Q. Han, Z.-Y. Wang, S. Sun, J.-X. Guo, X. Huang and X.-Y. Liu, *ACS Mater. Lett.*, 2025, **7**, 393–400.
40 C.-Q. Han, X. Sun, X. Liang, L. Wang, H. Hu and X.-Y. Liu, *J. Mater. Chem. C*, 2023, **11**, 12000–12006.
41 C. Zhu, C. Gong, D. Cao, L. Ma, D. Liu, L. Zhang, Y. Li, Y. Peng and G. Yuan, *Angew. Chem., Int. Ed.*, 2025, **64**, e202504348.
42 H. Xu, S. Xia, C. Li, Y. Li, W. Xing, Y. Jiang and X. Chen, *Angew. Chem., Int. Ed.*, 2024, **63**, e202405476.
43 I. Heckelmann, Z. Lu, J. C. A. Prentice, F. Auras, T. K. Ronson, R. H. Friend, J. R. Nitschke and S. Feldmann, *Angew. Chem., Int. Ed.*, 2023, **62**, e202216729.
44 H. Wang, C. Yang, F. Chen, G. Zheng and Q. Han, *Angew. Chem., Int. Ed.*, 2022, **61**, e202202328.
45 F. J. Uribe-Romo, J. R. Hunt, H. Furukawa, C. Klöck, M. O'Keeffe and O. M. Yaghi, *J. Am. Chem. Soc.*, 2009, **131**, 4570–4571.
46 H. Lyu, C. S. Diercks, C. Zhu and O. M. Yaghi, *J. Am. Chem. Soc.*, 2019, **141**, 6848–6852.
47 A. Acharjya, P. Pachfule, J. Roeser, F. Schmitt and A. Thomas, *Angew. Chem., Int. Ed.*, 2019, **58**, 14865–14870.
48 E. Jin, M. Asada, Q. Xu, S. Dalapati, M. A. Addicoat, M. A. Brady, H. Xu, T. Nakamura, T. Heine, Q. Chen and D. Jiang, *Science*, 2017, **357**, 673–676.
49 J. Guo, Y. Xu, S. Jin, L. Chen, T. Kaji, Y. Honsho, M. A. Addicoat, J. Kim, A. Saeki, H. Ihee, S. Seki, S. Irle, M. Hiramoto, J. Gao and D. Jiang, *Nat. Commun.*, 2013, **4**, 2736.
50 X. Chen, M. Addicoat, S. Irle, A. Nagai and D. Jiang, *J. Am. Chem. Soc.*, 2013, **135**, 546–549.
51 X. Chen, M. Addicoat, E. Jin, L. Zhai, H. Xu, N. Huang, Z. Guo, L. Liu, S. Irle and D. Jiang, *J. Am. Chem. Soc.*, 2015, **137**, 3241–3247.
52 J. L. Segura, S. Royuela and M. Mar Ramos, *Chem. Soc. Rev.*, 2019, **48**, 3903–3945.
53 N. Huang, R. Krishna and D. Jiang, *J. Am. Chem. Soc.*, 2015, **137**, 7079–7082.
54 A. Nagai, Z. Guo, X. Feng, S. Jin, X. Chen, X. Ding and D. Jiang, *Nat. Commun.*, 2011, **2**, 536.
55 L. Chen, K. Furukawa, J. Gao, A. Nagai, T. Nakamura, Y. Dong and D. Jiang, *J. Am. Chem. Soc.*, 2014, **136**, 9806–9809.
56 N. Huang, X. Chen, R. Krishna and D. Jiang, *Angew. Chem., Int. Ed.*, 2015, **54**, 2986–2990.
57 N. Huang, L. Zhai, D. E. Coupry, M. A. Addicoat, K. Okushita, K. Nishimura, T. Heine and D. Jiang, *Nat. Commun.*, 2016, **7**, 12325.
58 T. Banerjee, F. Haase, S. Trenker, B. P. Biswal, G. Savasci, V. Duppel, I. Moudrakovski, C. Ochsenfeld and B. V. Lotsch, *Nat. Commun.*, 2019, **10**, 2689.
59 H. L. Nguyen, C. Gropp and O. M. Yaghi, *J. Am. Chem. Soc.*, 2020, **142**, 2771–2776.
60 Y. Zeng, R. Zou, Z. Luo, H. Zhang, X. Yao, X. Ma, R. Zou and Y. Zhao, *J. Am. Chem. Soc.*, 2015, **137**, 1020–1023.
61 X. Chen, M. Addicoat, E. Jin, H. Xu, T. Hayashi, F. Xu, N. Huang, S. Irle and D. Jiang, *Sci. Rep.*, 2015, **5**, 14650.
62 X.-T. Li, J. Zou, T.-H. Wang, H.-C. Ma, G.-J. Chen and Y.-B. Dong, *J. Am. Chem. Soc.*, 2020, **142**, 6521–6526.
63 K. Wang, Z. Jia, Y. Bai, X. Wang, S. E. Hodgkiss, L. Chen, S. Y. Chong, X. Wang, H. Yang, Y. Xu, F. Feng, J. W. Ward and A. I. Cooper, *J. Am. Chem. Soc.*, 2020, **142**, 11131–11138.
64 P.-L. Wang, S.-Y. Ding, Z.-C. Zhang, Z.-P. Wang and W. Wang, *J. Am. Chem. Soc.*, 2019, **141**, 18004–18008.
65 Q. Guan, L.-L. Zhou and Y.-B. Dong, *J. Am. Chem. Soc.*, 2023, **145**, 1475–1496.
66 M. Hao, Y. Xie, M. Lei, X. Liu, Z. Chen, H. Yang, G. I. N. Waterhouse, S. Ma and X. Wang, *J. Am. Chem. Soc.*, 2024, **146**, 1904–1913.
67 H. Wu, L. Li, H. Chen, Y. Xing, Z. Wang, C. Zhang and X. Long, *Angew. Chem., Int. Ed.*, 2024, **63**, e202410719.
68 Y. Zhang, Z. Qiao, R. Zhang, Z. Wang, H. Wang, J. Zhao, D. Cao and S. Wang, *Angew. Chem., Int. Ed.*, 2023, **62**, e202314539.
69 M. Liu, C. Cui, S. Yang, X. Yang, X. Li, J. He, Q. Xu and G. Zeng, *Angew. Chem., Int. Ed.*, 2024, **63**, e202401750.
70 Q. Cheng, S. Liu, Y. He, M. Wang, H. Ji, Y. Huan, T. Qian, C. Yan and J. Lu, *Nat. Commun.*, 2025, **16**, 3717.
71 P. Das, G. Chakraborty, J. Roeser, S. Vogl, J. Rabeah and A. Thomas, *J. Am. Chem. Soc.*, 2023, **145**, 2975–2984.
72 P. Das, G. Chakraborty, J. Yang, J. Roeser, H. Küçükkeçeci, A. D. Nguyen, M. Schwarze, J. Gabriel, C. Penschke, S. Du, V. Weigelt, I. E. Khalil, J. Schmidt, P. Saalfrank, M. Oschatz, J. Rabeah, R. Schomäcker, F. Emmerling and A. Thomas, *Adv. Energy Mater.*, 2025, 2501193.
73 K.-H. Xie, G.-B. Wang, F. Huang, F. Zhao, J.-L. Kan, Z.-Z. Chen, L. Cai, S.-L. Han, Y. Geng and Y.-B. Dong, *Nat. Commun.*, 2025, **16**, 3493.
74 C. Yuan, S. Fu, X. Kang, C. Cheng, C. Jiang, Y. Liu and Y. Cui, *J. Am. Chem. Soc.*, 2024, **146**, 635–645.
75 M. Lei, Y. Xue, L. Gan, B. Li, Y. Lu, Q. Yang, W. Wang, S. Wang, Q. Su and Q. Wu, *Mol. Catal.*, 2025, **577**, 114976.
76 J.-R. Wang, K. Song, T.-X. Luan, K. Cheng, Q. Wang, Y. Wang, W. W. Yu, P.-Z. Li and Y. Zhao, *Nat. Commun.*, 2024, **15**, 1267.
77 M. Traxler, S. Reischauer, S. Vogl, J. Roeser, J. Rabeah, C. Penschke, P. Saalfrank, B. Pieber and A. Thomas, *Chem.–Eur. J.*, 2023, **29**, e202202967.
78 L.-L. Zhou, Q. Guan, W. Zhou, J.-L. Kan and Y.-B. Dong, *Chem. Sci.*, 2023, **14**, 3642–3651.